ZIRAT12 Annual Report

Authors

Alfred Strasser
Aquarius Services, Sleepy Hollow, NY, USA

Ron Adamson
Zircology Plus, Fremont, CA, USA

Brian Cox
University of Toronto, ON, Canada

Friedrich Garzarolli
Erlangen, Germany

Peter Rudling
ANT International, Skultuna, Sweden

George Sabol
Export, PA, USA

A.N.T. INTERNATIONAL®

● October 2007
Advanced Nuclear Technology International
Krongjutarvägen 2C, SE-730 50 Skultuna
Sweden

info@antinternational.com
www.antinternational.com

Disclaimer

The information presented in this report has been compiled and analysed by Advanced Nuclear Technology International Europe AB (*ANT* International) and its subcontractors. *ANT* International has exercised due diligence in this work, but does not warrant the accuracy or completeness of the information. *ANT* International does not assume any responsibility for any consequences as a result of the use of the information for any party, except a warranty for reasonable technical skill, which is limited to the amount paid for this assignment by each *ZIRAT* programme member.

Acronyms and explanations

ABB	ASEA Brown Boveri
ACRS	Advisory Committee on Reactor Safety
AL	Air Cool
ANL	Argonne National Laboratory
ANSYS	a finite element code
ANT	Advanced Nuclear Technology
AOA	Axial Offset Anomaly
APSR	Axial Power Shaping Rods
AR	Annual Report
ASTM	American Society for Testing and Materials
ATR	Advanced Test Reactor
BEP	Bottom End Plug
BQ	Beta-Quenched
BW	Basket-Weave
BWR	Boiling Water Reactor
CANDU	Canadian Deuterium Uranium
CB	Control Blade
CE	Combustion Engineering
CEA	Commissariat à l'Energie Atomique
CFR	Code of Federal Regulations
CIPS	*CRUD* Induced Power Shifts
CP	Cathcart-Pawel
CPR	Critial Power Ratio
CPSES	Comanche Peak Steam Electric Station
CRUD	Chalk River Unidentified Deposits
CSED	Critical Strain Energy Density
CTFF	Critical to Flawless Fuel
CWSR	Cold Work and Stress Relieved
CWSRA	Cold Work and Stress Relieved Annealed
CZP	Cold Zero Power
DBT	Ductile to Brittle Transitions
DCP	Distinctive CRUD Pattern
DFBN	Debris Filter Bottom Nozzle
DH	Dissolved Hydrogen
DHC	Delayed Hydride Cracking
DNBR	Departure from Nucleate Boiling Ratio
DSC	Differential Scanning Calorimetry
DTA	Differential Thermal Analysis
DX	Duplex
EBSD	Electron Back-Scattered Diffraction
ECBE	Effective Control Blade Exposure
ECCS	Emergency Core Cooling System
ECR	Equivalent Cladding Reacted
ECT	Eddy Current Testing
EDC	Expansion due to Compression Test
EDF	Electricité de France
EDS	Energy Dispersive X-Ray Spectroscopy
EFPD	Effective Full Power Days
EFPY	Effective Full Power Years
EIS	Environments by Impedance Spectroscopy
ELS	Extra-Low Sn
EPMA	Electron Probe Micro Analysis
ERDA	Elastic Recoil Detection Analysis
FA	Fuel Assembly
FC	Furnace Cool
FCI	Fuel Condition Index
FDI	Fuel Duty Index
FMEA	Failure Modes and Effects Analysis
FRED	Fuel Reliability Data Base

GNF	Global Nuclear Fuel
GT	Guide Tube
GTAW	Gas Tungsten Arc Welding
GTRF	Grid-to-Rod Fretting
HANA	High performance Alloy for Nuclear Application
HBR	HB Robinson
HDCI	High Duty Core Index
HFP	Hot Full Power
HPA	High Performance Alloy
HPF	Hydrogen Pick-Up
HPUF	Hydrogen Pickup Fraction
HWC	Hydrogen Water Chemistry
IAEA	International Atomic Energy Agency
ID	Inner Diameter
IFM	Intermediate Flow Mixing
IGA	Intergranular Attack
INL	Idaho National Laboratory
IRI	Incomplete Reactor Insertions
IT	Instrument Tube
IZNA	Information on Zirconium Alloys
JIT	Just In Time
KAERI	Korea Atomic Energy Research Institute
KKG	Kernkraftwerk Gundremmingen
KKL	Kernkraftwerk Leibstadt
KKP	Kernkraftwerk Philippsburg
L	Laves phase
LBLOCA	Large Break Loss Of Coolant Accident
LHGR	Linear Heat Generation Rate
LK	Låg corrosion (Low Corrosion in Swedish)
LOCA	Loss of Coolant Accident
LTA	Lead Test Assemblies
LUA	Lead Use Assemblies
LWR	Light Water Reactor
MDA	Mitsubishi Developed Alloy
MELLA	Maximum Extended Load Line Analysis
MHI	Mitsubishi Heavy Industries
MIMAS	Micronized Master Blend route
MOX	Mixed OXide
NDA	New Developed Alloy
NFIR	Nuclear Fuel Industry Research
NMC	Noble Metal Chemistry
NMCA	Noble Metal Chemical Addition
NRC	Nuclear Regulatory Commission
NSRR	Nuclear Safety Research Reactor
OD	Outer Diameter
OLNC	On-Line NobleChem
PAW	Plasma Arc Weldin
PCI	Pellet Cladding Interaction
PCMI	Pellet Cladding Mechanical Interaction
PGP	Particle Growth Parameter
P-Grid	Protective Grid
PIE	Post-Irradiation Examinations
PR	Partially Recristallized
PRX	Partial Recrystallization
PRXA	Partially Recrystallized Condition
PS	Power Suppression
PSCC	Primary Stress Corrosion Cracking
PSI	Paul Schrerrer Institute
PST	Power Suppression Testing
PT	Pressure Tube
PWR	Pressurised Water Reactor
QC	Quality Control

RBMK	Reaktor Bolshoi Mozhnosti Kanalov (in English Large Boiling Water Channel type reactor)
RCT	Ring Compression Rest
RDA	Rod Drop Accident
REA	Rod Ejection Accident
RFA	Robust Fuel Assembly
RIA	Reactivity Initiated Accident
RIL	Research Information Letter
RPN	Risk Priority Number
RT	Room Temperature
RTN	Removable Top Nozzle
RX	Recrystallised
RXA	Recrystallised Annealed
SAD	Selected Area electron Diffraction
SBR	Binderless Route
SCC	Stress Corrosion Cracking
SEM	Scanning Electron Microscopy
SNOC	Southern Nuclear Operating Company
SOCAP	Second Order Cumulative Annealing Parameter
SONGS	San Onofre
SPP	Second Phase Particle
SR	Stress Relieved
SRA	Stress Relieved Annealed
SRP	Standard Review Plan
STR	Special Topic Report
TCE	Total Circumferential Elongation
TEM	Transmission Electron Microscopy
TEP	ThermoElectric Power
TMI	Three Mile Island
TMT	ThermoMechanical Treatment
TPC	Taiwan Power Co
TSS	Terminal Solid Solubility
TU	TRANSURANUS
TVA	Tennessee Valley Authority
TXU	TeXas Utilities
UE	Uniform Elongation
UOX	Uranium OXide
UT	Ultrasonic Testing
UTS	Ultimate Tensile Strength
W	Westinghouse
WQ	Water Quench
VVER	Voda Voda Energo Reactor (Russian type PWR)
XRD	X-Ray Diffraction
YS	Yield
ZIRAT	ZIRconium Alloy Technology
ZIRLO	ZIRconium Low Oxidation

Unit conversion

TEMPERATURE

°C + 273.15 = K

°C*1.8 +32 = °F

T(K)	T(°C)	T(°F)
273	**0**	32
289	16	61
298	25	77
373	**100**	212
473	**200**	392
573	**300**	572
633	360	680
673	**400**	752
773	**500**	932
783	510	950
793	520	968
823	550	1022
833	560	1040
873	**600**	1112
878	605	1121
893	620	1148
923	650	1202
973	**700**	1292
1023	750	1382
1053	780	1436
1073	**800**	1472
1136	863	1585
1143	870	1598
1173	**900**	1652
1273	**1000**	1832
1343	1070	1958
1478	1204	**2200**

DISTANCE

x (µm)	x (mils)
0.6	0.02
1	0.04
5	0.20
10	0.39
20	0.79
25	0.98
25.4	**1.00**
100	3.94

PRESSURE

bar	MPa	psi
1	0.1	14
10	**1**	142
70	7	995
70.4	7.04	**1000**
100	10	1421
130	13	1847
155	15.5	2203
704	70.4	**10000**
1000	100	14211

MASS

kg	lbs
0.454	**1**
1	2.20

STRESS INTENSITY FACTOR

MPa√m	ksi√inch
0.91	**1**
1	1.10

Radioactivity

1 Sv = 100 Rem

1 Ci = 3.7 x 1010 Bq = 37 GBq

1 Bq = 1 s^{-1}

Contents

1 Introduction (Peter Rudling)

The objective of the Annual Review of Zirconium Alloy Technology (*ZIRAT*) is to review and evaluate the latest developments in zirconium alloy technology as they apply to nuclear fuel design and performance.

The objective is met through a review and evaluation of the most recent data on zirconium alloys and to identify the most important new information and discuss its significance in relation to fuel performance now and in the future. Included in the review are topics on materials research and development, fabrication, component design, and in-reactor performance.

Within the *ZIRAT12* Program, the following technical meetings were covered:

- Jahrestagung Kerntechnik, May 2007.
- Utility conference, Chicago, June 19-22, 2007.
- American Society for Testing and Materials (*ASTM*) Zr Conference, Sunriver, Oregon, USA, June 25-28, 2007.
- 19th International Conference on Structural Mechanics in Reactor Technology, Toronto, August 12-17, 2007.
- Thirteenth International Conference on Environmental Degradation of Materials in Nuclear Power Systems - Water Reactors, Whistler, British Columbia, August 19-24, 2007, Whistler, British Columbia, August 19-24, 2007.
- 7th International Conference on Voda Voda Energo Reactor (*VVER*) Fuel Performance, Modelling and Experimental Support, Albena near Varna, Bulgaria 17 - 21 Sep 2007.
- ANS Light Water Reactor (*LWR*) Fuel Performance Conference, San Francisco, Sept. 30- Oct. 3, 2007
- PATRAM Conference, October 2007, Miami, Florida

The extensive, continuous flow of journal publications is being monitored by several literature searches of world-wide publications and the important papers are summarised and critically evaluated. This includes the following journals:

- Journal of Nuclear Materials,
- Nuclear Engineering and Design,
- Kerntechnik
- Metallurgical and Materials Transactions A
- Journal of Alloys and Compounds
- Canadian Metallurgical Quarterly
- Journal de Physique IV
- Journal of Nuclear Science and Technology
- Nuclear Science & Engineering
- Nuclear Technology

The primary issues addressed in the review and this report are zirconium alloy research and development, fabrication, component design, ex- and in-reactor performance including:

- Regulatory bodies and utility perspectives related to fuel performance issues, fuel vendor developments of new fuel design to meet the fuel performance issues.
- Fabrication and quality control of zirconium manufacturing, zirconium alloy systems.
- Mechanical properties and their test methods (that are not covered in any other section in the report).
- Dimensional stability (growth and creep).
- Primary coolant chemistry and its effect on zirconium alloy component performance.
- Corrosion and hydriding mechanisms and performance of commercial alloys.

- Cladding primary failures.
- Post-failure degradation of failed fuel.
- Cladding performance in postulated accidents (Loss of Coolant Accident (*LOCA*), Reactivity Initiated Accident (*RIA*)).
- Dry storage.
- Potential burnup limitations.
- Current uncertainties and issues needing solution are identified throughout the report.

Background data from prior periods have been included wherever needed. Most data are from non-proprietary sources; however, their compilation, evaluations, and conclusions in the report are proprietary to *ANT* International and *ZIRAT* members as noted on the title page.

The information within the *ZIRAT12* Program is either retrieved from the open literature or from proprietary information that *ANT* International has received the OK from the respective organisation to provide this information within the *ZIRAT* program.

The authors of the report are Dr. Ron Adamson, Brian Cox, Professor Emiritus, University of Toronto; Mr. Al Strasser, President of Aquarius and, Mr. Peter Rudling, President of *ANT* International, Mr. Friedrich Garzarolli, Dr. Rolf Riess and Mr. George Sabol.

The work reported herein will be presented in three Seminars: one in Clearwater Beach, Florida, on February 4- February 6, 2008 one in Valetta, Malta on February 18-20, 2008 and one in Japan in 2008.

The Term of *ZIRAT12* started on February 1, 2007 and ends on January 31, 2008.

2 Burnup achievements and fuel performance issues (Alfred Strasser)

2.1 Trends in fuel operating conditions

2.1.1 General trends

The desire for further improvements in operating economics and reliable fuel performance has resulted in significant advances in materials technology and software for modeling fuel performance. These advances have been used to increase the demands on fuel performance levels and to put pressure on the regulatory bodies to license operations to ever higher burnups. The types of changes in *LWR* operating methods to achieve improved safety and economics have not changed in the past year and still include:

- Annual fuel cycles extended to 18 and 24 months.
- Discharge burnups increased from mid-30 to mid-50 GWD/MT batch average exposures by higher enrichments, increased number of burnable absorbers in the assemblies and in Pressurised Water Reactor (*PWR*s) higher Li and B levels in the coolant.
- Plant power uprates that ranged from 5 to 20%.
- More aggressive fuel management methods with increased enrichment levels and peaking factors.
- Reduced activity transport by Zn injection into the coolant.
- Improved water chemistry controls and increased monitoring.
- Component life extension with Hydrogen Water Chemistry (*HWC*) and Noble Metal Chemistry (*NMC*) in Boiling Water Reactor (*BWR*s).

2.1.2 Fuel cycle lengths

The trend for increased fuel cycle lengths has come to a near "equilibrium" in the US with *PWR*s operating at an average of 500 Effective Full Power Days (*EFPD*) per cycle and *BWR*s an average of over 600 *EFPD* per cycle. Maxima are about 700 days for *PWR*s and 730 days for *BWR*s, Figure 2-1. Nearly all the US *BWR*s are trending toward 24 month cycles. The older, lower power density *PWR*s have implemented the 24 month cycles, but fuel management limitations, specifically reload batch sizes required, have limited implementation of 24 month cycles in the high power density plants. The economics of 24 month cycles tend to become plant specific since they depend on the balance of a variety of plant specific parameters. The potential economic gains for cycle extension have decreased in the US since the downtimes for reloading and maintenance procedures have been significantly reduced.

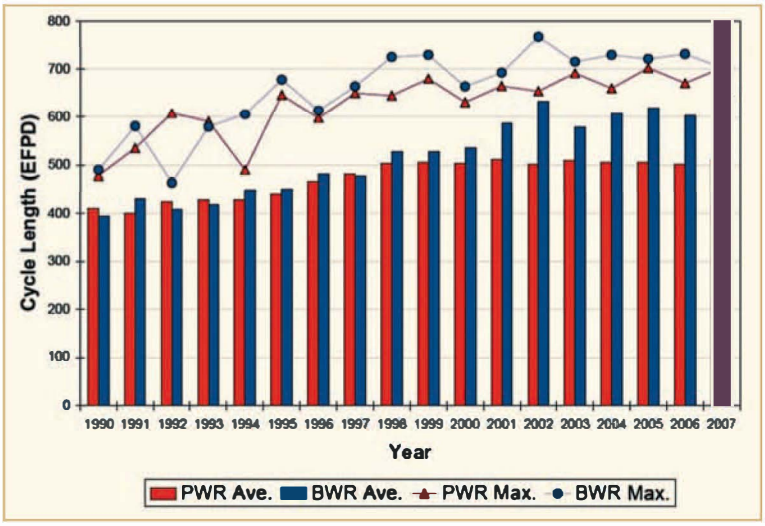

Figure 2-1: Cycle Length Trends in the US (Kucuk, 2007).

Other countries that historically have had only one power demand peak in the winter compared to the two summer and winter power peaks in the US are also trending toward longer cycles as a result of changes in economics, maintenance practices and licensing procedures. *PWR*s are trending toward 18 month cycles in France (900 and 1300 MW plants), the UK (Sizewell B) and Germany. Japan is planning to increase cycle lengths in several steps, first to 15 months which does not require relicensing, then to 18 and 24 months which will require relicensing.

2.1.3 Burnup extension

Improved economics of the fuel cycle are the incentives for extended burnups, and include the decreased amount of spent fuel assemblies to be handled. The economics of decreased assemblies could be impacted by the much longer cooling times required in spent fuel pools prior to on-site dry storage or transport to a storage facility as noted later. The average batch burnups in US *PWR*s are approaching 50 GWD/MT and in US *BWR*s in the mid-40GWD/MT, Figure 2-2. Some *PWR*s exceed the 50 GWD/MT batch burnups, as in one example to 57 GWD/MT.

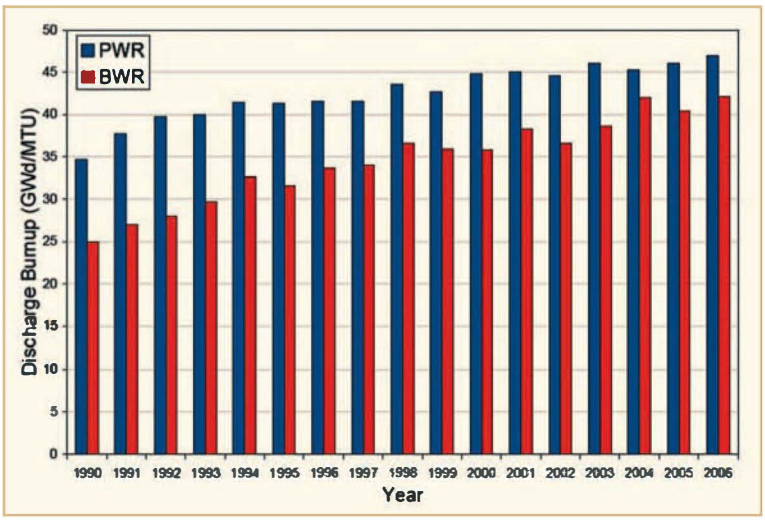

Figure 2-2: Average Discharged Assembly Burnup Trends in the US (Kucuk, 2007).

Some European plants operated in the 50-55 GWD/MT batch burnup range and have designed to go to 58-60 GWD/MT in their current cycles in both *PWR*s and *BWR*s. This is feasible, in part, due to their greater margin to regulatory limits. The maximum burnup Lead Use Assemblies (*LUA*s) are in the range of 67 – 75 GWD/MT for both reactor types.

The *VVER*-440 fuel is up to 57 GWD/MT assembly burnup with plans to got to 65 GWD/MT. The *VVER*-1000 fuel is up to 55 GWD/MT assembly burnup with plans to go to 68 GWD/MT (Molchanov, 2007).

The Japanese are planning to raise current *BWR* 45 GWD/MT batch average burnup to 50 GWD/MT without exceeding the 55 GWD/MT peak assembly burnup regulatory limit for 9x9 "Step 2" fuel (Itagaki, 2007). This will be done in conjunction with cycle extension from their current 13 month to future 16 or 19 month cycles. The *PWR* assembly burnups will also be raised to 55 GWD/MT for all rod arrays.

The burnups are currently limited by the regulatory agencies more than by technical limitations, except for *LUA*s and rods. Some of the current regulatory limits are in GWD/MT:

USA	62.5	peak rod	Korea	60 peak rod
Belgium	55	UO_2 assembly	Netherlands	60 peak rod
	50	*MOX* assembly	Sweden	60 assembly
Finland	45	assembly		64 rod
France	52	assembly	Switzerland	75 peak pellet
Germany	65	assembly	Taiwan	60 peak rod (*PWR*)
Japan	55	UO_2 assembly		54 peak assembly (*BWR*)
	(66	peak rod)	UK	55 peak pellet
	45	*MOX* assembly		

Economic analyses reported in past *ZIRAT* reports indicated that economic incentives for extending burnups beyond the 60-70 GWD/MT batch average range will disappear and that other incentives will be needed to go beyond this level.

The biggest block to increasing burnup is the essentially universal regulatory limit on 5.00% initial uranium enrichment. Analyses reported in *ZIRAT*11 for a variety of reactors that included *PWR*s and *BWR*s showed that a 5% enrichment will provide up to 55 GWD/MT in a *VVER* and about 63 GWD/MT in a GE *BWR assembly* average burnup. Advanced, sophisticated fuel management methods can probably raise this close to 70 GWD/MT, but are unlikely to exceed this level. The cost of equipping and licensing the industry to handle enrichments greater than 5% would be very great and time consuming; and for that reason such a move is not being considered for the foreseeable future.

In spite of this negative outlook by most of the Industry, there is a Japanese development program for using erbia burnable absorber rods with >5% enriched UO_2 and licensing them based on "erbia credit" (Itagaki, 2007).

2.1.4 Fuel cycle economics

Fuel cycle analyses reported in past *ZIRAT* reports have shown that the fuel cycle cost vs. burnup curve is essentially flat or start increasing in cost in the 60-70 GWD/MT batch average burnup range. The recent cost increases in uranium ore and enrichment will start raising the fuel cycle costs at a lower burnup than before. The uranium prices have risen to over \$100/lb of U_3O_8 and the enrichment costs over \$140/ kg SWU, Figure 2-3.

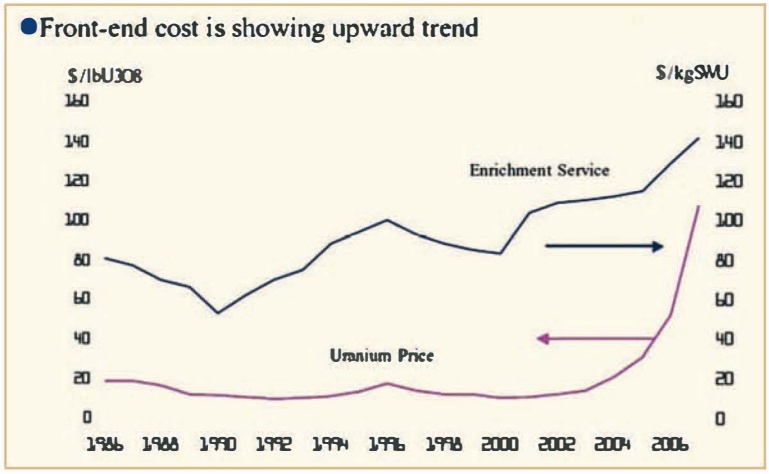

Figure 2-3: Price Index Trends of Uranium & Enrichment (Suzuki, 2007).

Up-to-date estimates on their effect on fuel cycle costs have not been published, but a simple example can be made by adjusting the most recent estimates published (Gregg, 2005), reviewed in *ZIRAT11* and shown on Figure 2-4. Assuming the case for a burnup of 60 GWD/MT there is an increase for uranium ore from \$25 used by Gregg to \$100 or a factor of 4, raising the uranium cost from 0.8 on curve (5) to 3.2 \$/MWhr. The enrichment costs went from \$90 used by Gregg to about \$140 an increase of 33%, raising the enrichment cost from 1.75 on curve (4) to 2.33 \$/MWhr. The original total fuel cost from adding up all the cost component curves at 60 GWD/MT is 4.8 \$/MWHr and adding the uranium and the enrichment cost increases the total fuel cost to 8.58 \$/MWHr (equivalent to mills/kwhr), a significant 79% increase in fuel cycle cost for the example cited. This increase will make further extensions to burnup less attractive than they were before.

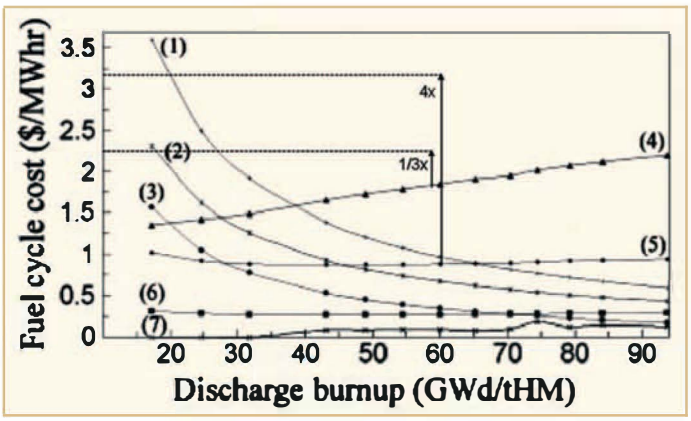

Figure 2-4: Typical Levelized Fuel Cost vs. Burnup Assuming Constant Unit Cost with Enrichment: (1) conditioning and final disposal costs, (2) fabrication costs, (3) transportation costs, (4) enrichment costs, (5) ore costs, (6) conversion costs, and (7) gadolinia costs (Gregg, 2005).

A current cost estimate by an anti-nuclear group presents a pessimistic view of the overall generation economics of 7.4 to 11.1¢/kWh and fuel cycle costs of 1.3 to 1.7 ¢/kWh (13-17 mills/kwhr), Table 2-1 and Table 2-2. Their cost estimate is based on a 75% capacity factor which has been exceeded for some time and is more like 90%, a factor that would make a significant difference in their generation cost. The US capacity factor trend is compared to that of other countries in Figure 2-5.

There is a need for an updated fuel cycle and total generating cost estimate as a function of burnup including all the parameters that affect these costs. A sensitivity study of the back-end costs would be particularly important where the uncertainty of the permanent storage date could raise the cost of dry storage requirements. Another factor to consider is the spent fuel pool that may run short of capacity due to the increased cooling requirements for high burnup assemblies (even though there are less of them) and may require new pool construction in some cases. The Goesgen plant in Switzerland is a good example. A sensitivity study could cover the broad range of plants and their specific requirements.

Table 2-1: New Nuclear Cost Assumption.

Assumptions (2007 $s)	Low case	High case
Overnight cost	$2430/kW	$2950/kW
Capital cost, inc. interest*	$3000/kW	$4000/kW
Capacity factor	90 percent	75 percent
Financial	8% debt, 12% equity, 50/50	8% debt, 15% equity, 50/50
Depreciation	15 year accelerated	15 year accelerated
Fixed O&M	5 mills/kWh	5 mills/kWh
Variable O&M	5 mils/kWh	5 mils/kWh
Fuel	1.2 cents/kWh	1.8 cents/kWh
Grid intergration	$20/kW-year	$20/kW-year

* 3.000/kW assumes 0% real escalation and 5 year construction period;
4.000/kW assumes 3.3% real escalation, 6 year construction period.

Table 2-2: New-Nuclear Levelized Cost Estimate ($2007).

Cost category	Low case	High case
Capital costs	3.8	6.2
Fuel	1.3	1.7
Fixed O&M	1.9	2.7
Variable O&M	0.5	0.5
Total (levelized cents/kWh)	7.4	11.1

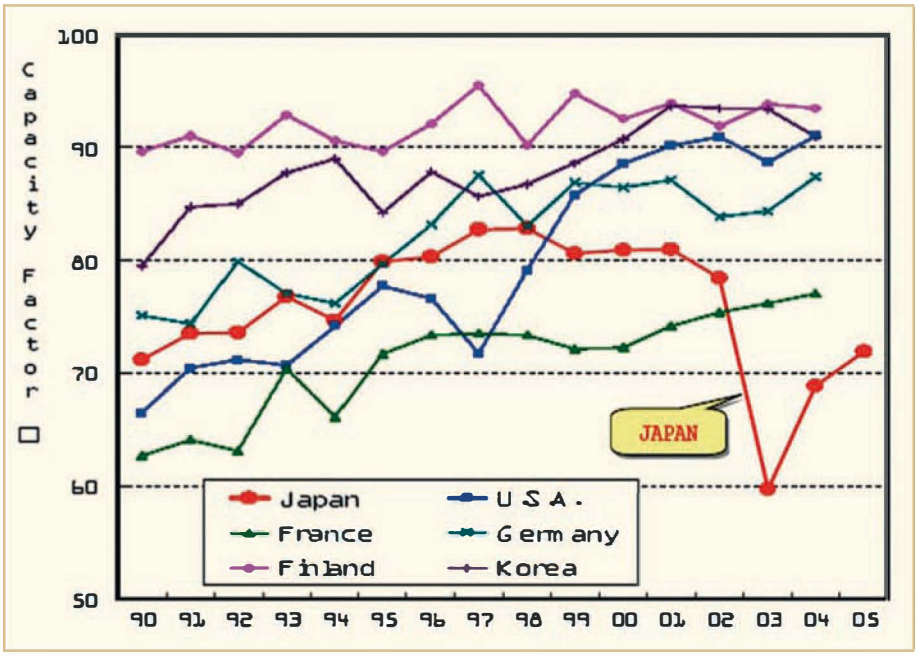

Figure 2-5: Comparison of Capacity Factors (Suzuki, 2007).

2.1.5 Power uprates

The power of the majority of the operating plants has been uprated, the maximum being 20%. While the fuel performance limits remain the same for the uprated conditions, the number of fuel assemblies operating at higher power change and the margin to the limits might be reduced. The effect of higher flow rates on hydraulic and water chemistry effects on the interaction with the fuel must also be considered. These changes have not affected the failure rate or apparently the fuel performance; however, it does increase the statistical probability of increasing power and burnup related factors on the fuel performance.

The most recent power uprates in the US are:

Approved (since the start of 2005, with percentage of thermal power increase)

Seabrook,	5.2	Palo Verde-1,	2.94	*Seabrook,*	1.7	*Beaver Valley-2,*	8.0
Indian Point-3,	4.85	Palo Verde-3,	2.94	*Ginna,*	16.8	*Browns Ferry-1,*	5.0
Waterford-3,	8.0	Vermont Yankee,	20.0	*Beaver Valley-1,*	8.0		

Applications under review (with percentage of thermal power increase)

Browns Ferry-1,	15.0	Calvert Cliffs-1,	1.3	Hope Creek,	15.0	Davis-Besse,	1.6
Browns Ferry-2,	15.0	Calvert Cliffs-2,	1.3	Susquehanna-1,	13.0	Millstone-3,	7.0
Browns Ferry-3,	15.0	Fort Calhoun,	1.5	Susquehanna-2,	13.0		

The most recent analyses of the effects of uprates on core power distribution were for the Kernkraftwerk Leibstadt (*KKL*) plant, a GE *BWR-6* (Ledergerber, 2007). The first uprate of the plant was 4.7% (3012 to 3138 MW) and the second uprate was 14.7% (3138 to 3600 MW). The second uprate was accompanied by the change from 8x8 to 10x10 fuel. The effect of the power uprates on the fuel assembly power census can be observed by comparing Cycle 13 with Cycle 15 for the first uprate and Cycles 17/18 to Cycles 19/21 for the second uprate, Figure 2-6. There is an increase in the number of assemblies at the highest Linear Heat Generation Rate (*LHGR*) range of 260-280 W/cm (7.9-8.5 kW/ft). The accompanying average rod *LHGR* can be up to 300 W/cm (9.1 kW/ft) and a peak rod range of 380-400 W/cm (11.6-12.2 kW/ft).

The batch average burnup was increased in the process, in conjunction with the improved fuel designs, to >52 GWD/MT, Figure 2-7. The part length rods of the new designs played a significant role in increasing the stability of the core which in turn could lead to the increasing operating flexibility by an expanded Global Nuclear Fuel (*GNF*) power flow map, Maximum Extended Load Line Analysis (*MELLA+*) (Figure 2-8), a feature that is taking a considerable time to get licensed in the US. The expanded power-flow map will facilitate operation at the uprated core powers as indicated on the figure.

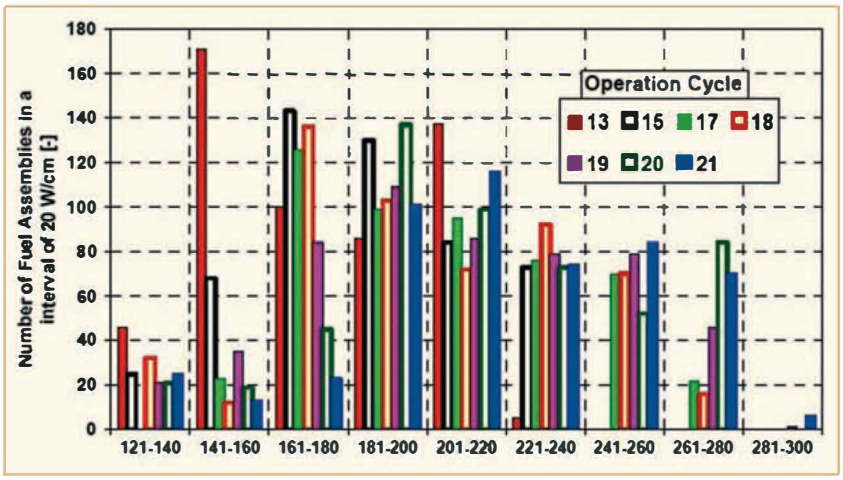

Figure 2-6: Impact of Power Up-Rate on Rod Power Density at *KKL* (Ledergerber, 2007).

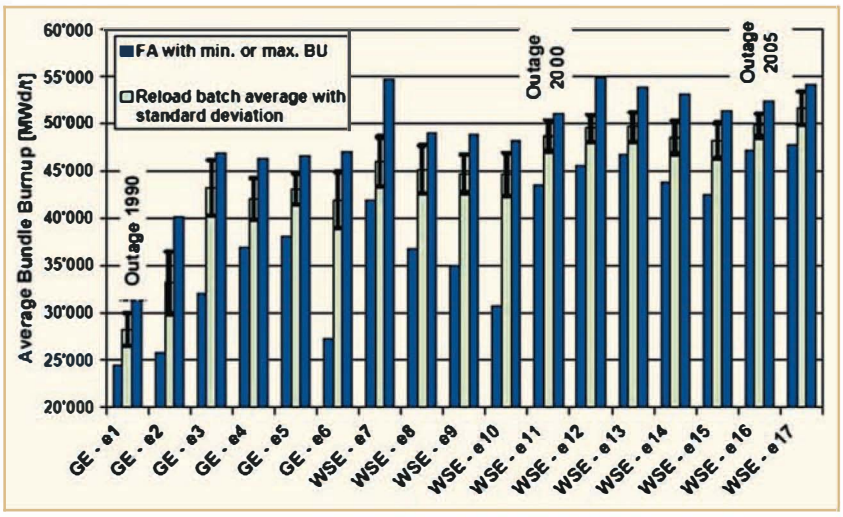

Figure 2-7: Average Discharge Burnup with Standard Deviation and Fuel Assembly Min.-Max. Burnup for Reload Batches at *KKL* (Ledergerber, 2007).

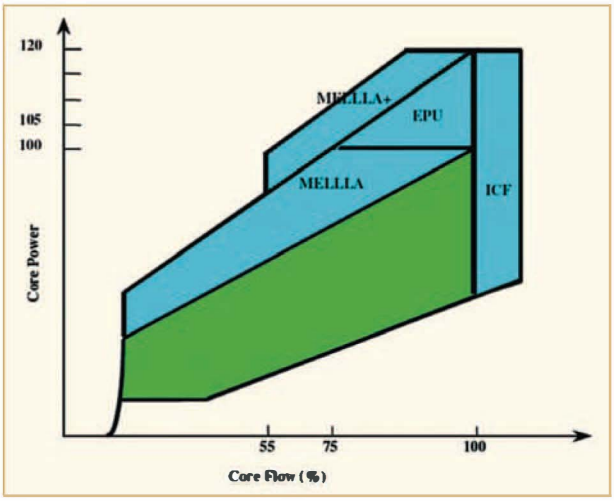

Figure 2-8: MELLLA+ Expanded Power-Flow Map for Uprated Plants (Schardt, 2007).

2.1.6 Water chemistry

High lithium operation

Increasing burnup, cycle lengths and enrichments levels, combined with the recommended high, 7.4 pH operation has increased the required lithium (Li) levels above the previously used 3.5 ppm concentrations. The potentially increased zirconium alloy corrosion levels due to increased Li levels has created a cautious approach to increasing the Li levels; the concentration of Li in high Chalk River Unidentified Deposits (*CRUD*) levels and/or in combination with nucleate boiling is of particular concern. The highest Li level used has been at the Comanche Peak Unit 2 (*CPSES* 2):

Cycle	Li (ppm)	pH	Days >3.5 ppm Li
7	<5	7.3	66
8	<6	7.4	334
9	<6	7.4	468

The cycles were 18 months long and the fuel accumulated 42-50 GWD/MT assembly burnup after 3 cycles.

Results from the first two cycles were reported in *ZIRAT*11 and the results from Cycle 9 are summarized here (Kargol, 2007). The *CPSES* 1 unit operated at <3.5 ppm Li and pH of 7.1-7.2 as a reference plant. The Li level history for each cycle in each plant is given in Figure 2-9.

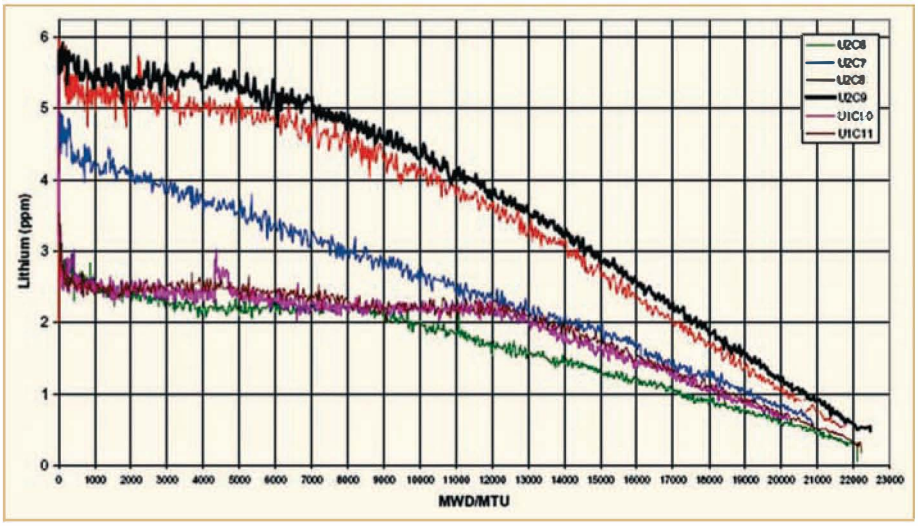

Figure 2-9: Lithium Histories in *CPSES* Units 1 and 2 (Kargol, 2007).

Oxide measurements after Cycle 7 indicated levels below the best estimate oxide levels for normal operation as well as decreased *CRUD* levels. The same assemblies operated at a higher power and nucleate boiling levels and oxide measurements indicated a 10% higher oxide thickness than expected for the highest duty rods, but also a significantly higher *CRUD* level. Significant scatter was also observed among the high duty rods, up to a factor of 2 in oxide thickness for rods with the same thermal history. The lack of *CRUD* brushing prior to the oxide measurements could also add to the uncertainties. Any Li effect could well be covered by a power effect.

The new data for Cycle 9 is the result of the examination of 8 assemblies that operated in *CPSES* 2 and 8 assemblies that operated as controls in CSPES 1. The cladding in all of the assemblies was ZIRconium Low Oxidation (*ZIRLO*). Oxide measurements (after *CRUD* brushing this time) showed significant scatter among the high duty rods. The highest oxide level was almost 60 μ but most were below 30 μ on fuel rods with similar thermal histories, Figure 2-10.

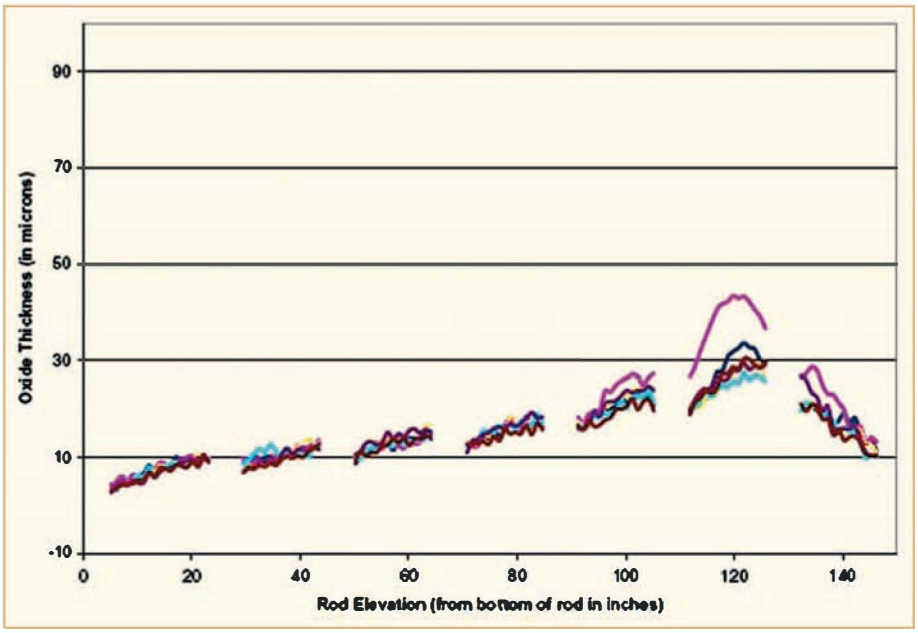

Figure 2-10: *ZIRLO* Oxide Measurement After Li <5 ppm, then Li <6 ppm for 3 Cycles (Kargol, 2007).

Comparison to a 2 cycle, high Li exposed rod and the 3 cycle, low Li rod from *CPSES* 1 (Figure 2-11) indicate they can be quite similar. This led to the conclusion that exposure time to Li and perhaps to Li levels is less significant than the exposure to power levels.

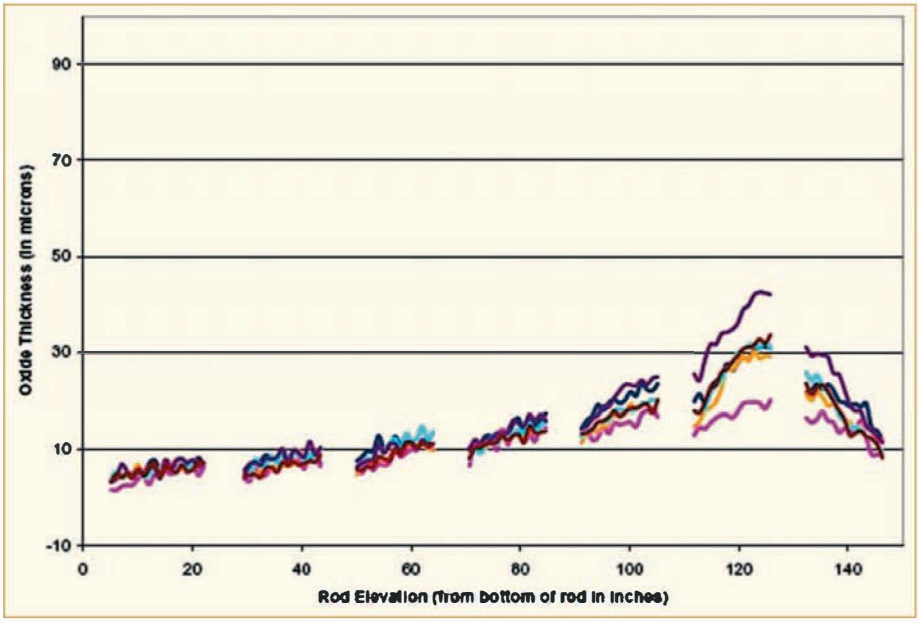

Figure 2-11: *ZIRLO* Oxide Measurement After 3 Cycles in *CPSES* Unit 1, Li <3.5 ppm (Kargol, 2007).

Diablo Canyon Units 1 and 2 have been operating at a Li level of up to 4.2 ppm for a pH of 7.2. Their oxide levels on *ZIRLO* are typically <25μ, lower than CSPES 2. This is attributed to the lower fuel duty and the presence of Intermediate Flow Mixers (*IFM*s) on their fuel assemblies that reduce the steaming rate, the parameter used for nucleate boiling levels (Kargol, 2007).

The conclusion of this work was that operation with up to 6 ppm Li does not have a significant effect on ZIRLO corrosion with the possible exception of some limited acceleration under conditions that existed in CPSES2.

It is of interest to note that North Anna is considering operation with >6.9 ppm Li.

Zinc injection

One of the successful innovations in operating methods has been zinc (Zn) injection into the coolant to reduce activity transport within the primary coolant systems of both *PWR*s and *BWR*s, without significantly affecting cladding corrosion, be it Zircaloy-4, *ZIRLO* or M5. The presence of Zn, however, promotes the deposit of a Zn containing spinel on the cladding probably in the form of $Ni_xZn_yFe_zO_4$, especially if sufficient Fe is present. While these *CRUD* deposits have not been observed to affect corrosion of the cladding, they are suspected of promoting boron deposits that can result in Axial Offset Anomaly (*AOA*s) also called *CRUD* Induced Power Shifts (*CIPS*s) in plants with subcooled nucleate boiling. A key question has therefore been the effect of Zn injection on cores with nucleate boiling and the experience of such plants with recently applied Zn injection.

A total of 15 *PWR* plants are injecting Zn in the US, of which 9 are doing it for dose rate reductions at the 2-7 ppb level, and 6 are injecting for structural material stress corrosion cracking at the 13-40 ppb level. Nearly all the *BWR*s have applied Zn injection.

The highest duty *PWR* plants in the US with Zn injection have been the Vogtle Units with a High Duty Core Index (*HDCI*) of about 175. Vogtle 1, Cycle 13 had evidence of an *AOA* during a Zn injection period and the Zn injection was shut off. Oxide measurements at the end of the cycle in the fall of 2006 showed that the oxide thickness of the cladding was normal including areas calculated to have nucleate boiling. *CRUD* scrape analyses showed a structure consistent with *AOA CRUD* samples of previous cycles. Vogtle 2, Cycle 12 operated with Zn injection increasing its levels from 5 to 10 to 15 ppb without an *AOA*. The fuel examination planned during the outage in March 2007 did not occur due to inspection equipment problems. (Loftin, Turnage, 2007).

As reported in *ZIRAT11* it is important to remember that Gösgen, a Siemens NSSS, the highest duty *PWR* with significant amount of nucleate boiling, has been injecting Zn since 2004 with no reported effects on the fuel cladding. They operate with relatively low levels of 28% enriched ^{10}B at 950 ppm B at the beginning of cycle, obviating *AOA*s combined with their insignificant *CRUD* levels.

2.2 High burnup fuel performance summary

2.2.1 High burnups achieved in utility power plants

The currently achieved burnup levels achieved in power plants are summarized in Table 2-3 for *PWR*s and Table 2-4 for *BWR*s based on publications during the past years and data provided by *ZIRAT* Members in response to our questionnaire on this topic. While the data are not complete, they represent a fair picture of the trends in the utilities of various countries that responded to the questionnaire or have published their data.

Table 2-3: Highest Burnup Achievements in *PWR*s.

	GWD/MT		
	Batch Ave.	Peak Assembly	Rod
USA (62 GWD/MT peak rod NRC limit)			
Wolf Creek, W RFA, ZIRLO	47	48.0	52.8
W RFA-2		48.0	
Callaway		54.6	
Watts Bar, Sequoyah	47.7	54.7	60.0
Diablo Canyon 1 & 2	54.0	58.0	62.0
Indian Point 2 & 3	52	57 limit	60 limit
Catawba, McQuire, all ZIRLO			57
Oconee, M5 clad, GTs	51.0	68.0	72
North Anna			
3LTAs, M5 clad		52.0	
1LTA, M5 clad		67.6	
1LTA, ZIRLO clad			72
Other US PWRs Mk-BW, M5 clad	50.0	67.6	72
W, RFA-2, ZIRLO clad	49.6	51.2	
Alliance LUA		48.9	
FINLAND			
Louisa 1 & 2, VVER-440	40.0	53.4 (E110) 51.4 (Zr4)	59.0 (E110) 56.9 (Zr4)
FRANCE (52 GWD/MT peak assy. regulatory limit)			
EdF plants, M5	47.0	51 UO_2	
		42 MOX	
LTAs in France and other countries with M5 clad		68 UO_2	80 UO_2
			60 MOX
GERMANY			
Biblis A & B	35-38 (56 planned)	41-47	48-50
Emsland	52 (62 planned)	62	68
Unterweser, M5 clad, HTP spacer	49	52	59
Isar 2, Duplex ELS 0.8 clad HTP sp.	56	59	62
LTA all M5		48	
BrokdorF, Duplex ELS 0.8 clad, HTP sp.	49.1	58.9	62.9
Grafenrheinfeld, DX Zr 2.5Nb, DZHPA-4, M5	53	58.3	61.4
Grohnde, Duplex ELS 0.8 clad, HTP sp.	49.1	58.9	62.9
Phillipsburg, FOCUS	51.9		
AFA 3G	53.1		
AFA 3G, MOX	53.4		
HTP	32.4		
HTP, MOX	53.9		
W	55.3		
LTA, all M5		51.8	
LTA, Zr1Nb+Fe+Sn		53.1	

Table 2-3 Highest Burnup Achievements in *PWR*s (Cont'd).

	GWD/MT		
	Batch Ave.	Peak Assembly	Rod
JAPAN			
Kansai plants, Step 1 fuel		48	
Step 2 LTA: ZIRLO MDA, NDA clad		55	
4 LTAs (Ohi4) NDA clad		52	60
LT rods (McGuire+R2), NDA clad			84
			91 (pellet)
(Vandellos), MDA and ZIRLO clad		>55	75
Future planning		70	
NETHERLANDS	48.9	54.9	57.6
RUSSIA			
WER-440s	45.3	56 (45-49 ave.)	58-60 66-68 pellet
WER-1000s		55.5 (40-49 ave.)	
Kalininskaya 1 LTA		62	71
SPAIN			
Almaraz 1	46.2	52.4	56.0
Almaraz 2	46.8	54.8	58.7
Trillo	50.2	57.4	61.7
SWEDEN			
Ringhals 2, W AEF+	45.3	47.1	
LTA Fragema AFA-3GAA		60.1	
Ringhals 3, Fragema AFA-3G	47.1	52.4	
LTA, Siemens HTP		57.2	
Ringhals 4, Fragema AFA-3G	46.2	51.8	
LTA, Fragema AFA-2G		50.3	
SWITZERLAND			
Gösgen, DXELS 0.8b	55 max.	55 ave.	59 ave.
LTA, DX HPA4		71.5	74.0
LTA, DX Zr2.5Nb			106.0
Beznau1, Focus 14*14 Duplex	58.0	60.0	65.0
Beznau2, Focus 14*14 Duplex	58.0	60.0	65.0
UK			
Sizewell	43.0	45.0	
UKRAINE			
Eleven WER-1000		49-50 (42-43 ave.)	

Table 2-4: Highest Burnup Achievements in *BWR*s.

	GWD/MT		
	Batch Ave.	Peak Assembly	Rod
USA			
Browns Ferry		49.0	55
			66 (pellet)
Grand Gulf, GE-11, P 6/7 clad	46.8	51.1	56.4
going to ATRIUM 10 non-liner			67.9 (pellet)
River Bend, GE-11, P 6/7 clad	47.3	51.5	55.3
			67.5 (pellet)
Fitzpatrick, Pilgrim	45-48		
Other US BWRs, GE-14	47.5	52.1 GE-11	
ATRIUM-10	43.1	53.0 GE-13	
FINLAND			
OL1, ATRIUM10B, LTP clad	45.0	40.0	43.0
LTA, GE-14		36.0	40.0
OL2, GE-12, P6 Triclad	45.0	40.0	43
SVEA 96 Optima		38.0	51
GERMANY			
KK Gundremmingen, UO_2	49	67-75	73-82
KK Gundremmingen, MOX	nearly 50 ave.	58 ave.	68 pellet
KK Isar 1	49.7 peak	53.3 peak	60 peak, LK3
Philipsbu 1			
Atrium 10B	52.8		
Atrium 10XP	11.8 (24.6)		
GE12	49.2	49	
SVEA 96 Optima 2	33.1 (43.1) (60 planned)		
JAPAN			
Fukushima Daini #1			
LTA 9x9 Step III, Zr2 liner clad		55	
LTA 9x9 Step III, HiFi clad		53	72 equiv. HiFi coupons
SPAIN			
Cofrentes, SVEA 96	44.6	49.7	60.3
			66.3 (pellet)
LTA, SVEA 96		53.0	63.4
			68.8 (pellet)
SWEDEN			
Ringhals 1, Atrium 10B		39.1	
Forsmark 1, GE-12	41.7	44.7	
Atrium 10B	42.9	41.7	
Forsmark 2, SVEA 96S	41.8	45.3	
2 LTAs, SVEA 96S		39.7	
2 LTAs, GE-14		41.3	
6 LTAs, Optima 2		40.7	
Forsmark 3, SVEA 100	42.4	43.8	
2 LTAs, SVEA 100		41.3	
4 LTAs, GE-14		38.9	
8 LTAs, ATRIUM 10B		39.1	
Oskarshamn 1, SVEA 96 Optima	27	33.0	
SVEA 64, LK2 + clad		43.1	48.3
Oskarshamn 2, SVEA 96, Optima 2	12	16.0	
ATRIUM 10B	41.0	48.0	
Oskarshamn 3, SVEA 96, Optima 2	45.0	49.0	53.8
SVEA 96, Optima 2	37.0	43.0	
SWITZERLAND			
2 LTAs, KKL SVEA96, LK3 clad		60+	68-73

The *highest burnup levels in PWRs* have been implemented in the US, Germany, Russia and Switzerland. The batch averages range between 47 and 58 GWD/MT with plans to go to 60-62 GWD/MT in Germany. The peak assemblies range between 48 and 72 GWD/MT and the peak rods between 53 and 105 GWD/MT burnup. The batch average burnup levels in the US plants have reached their maximum level permitted by the 62 GWD/MT max. rod exposure established by the Nuclear Regulatory Commission (*NRC*), until more data become available to justify increased regulatory burnup limits. The values above this level are in German, Russian and Swiss plants. The current examinations of US rods from Lead Test Assemblies (*LTA*s) in the 65 – 75 GWD/MT range are planned to justify the increase the current limit to 70 or 75 GWD/MT.

While the French *PWR*s are limited to 52 GWD/MT assembly average burnup by their regulatory body, the current goal of the industry is to increase the limit to 70 GWD/MT. Similarly, the Japanese utilities, while they have relatively conservative current burnup levels, have an irradiation program to raise this to 90-100 GWD/MT rod burnup.

The *LTA*s are usually exempt from regulatory limits and their highest peak rod burnups achieved have been in GWD/MT: 72 (US, Russia), 80 (France), 84 (Japan), 90 (Switzerland).

The peak burnups in GWD/MT achieved by the current *PWR* cladding materials have been:

		Batch	Assembly	Rod
ZIRLO		55	58	75
M5	:	53	68	80
E-110			62	72
Duplex, various	:	58	62	68
PCA2b		49	55	58
M-*MDA*				72

The *highest burnups in BWRs* are in the US, Germany, Spain and Switzerland. The batch averages range between 43 and 53 GWD/MT, peak assemblies between 51 and 62 GWD/MT and the peak rods between 55 and 73 GWD/MT. The burnup levels in *BWR*s are catching up to those of the *PWR*s in the US, probably because of the current *NRC* burnup limitation. Irradiation results of a variety of *BWR* vendor fuel designs in Kernkraftwerk Gundremmingen (*KKG*) and *KKL* to extended burnups are of significant interest in this regard when published.

The highest peak rod burnups achieved in *LTA*s have been in GWD/MT: 63 (Spain), 65 (US), 72 (Japan), 73 (Switzerland), 75 assembly (Germany).

The peak burnups achieved by the current cladding materials have been:

Zircaloy 2 (GWD/MT) : 49 batch, 53 assembly, 65 rod,
Low Corrosion in Swedish (*LK3*) (GWD/MT) : 47 batch, 53 assembly, 60 rod.

The assembly and rod burnups listed above were achieved without failures; however, fuel assemblies and materials do not have a perfect performance record up to these burnups levels and the related problems are summarized in Section 2.3 and discussed in detail in subsequent sections.

2.2.2 High burnup fuel examination results

2.2.2.1 Oxides

The development of *chromium oxide (Cr_2O_3) doped UO_2 fuel pellets* for *BWR*s and *PWR*s by AREVA is based on the following advantages that they can offer over standard UO_2 pellets (Delafoy, 2007):

- Improved Pellet Cladding Interaction (*PCI*) performance,
- Reduced fission gas release,
- Decreased chipping during fabrication,
- Decelerated washout characteristics.

The pellets contain about 0.16% Cr_2O_3, which increases their grain size to 50-60µ for improved fission gas release and increased viscoplasticity for greater margin to *PCI* failures. Fuel with the doped pellets have been irradiated for up to 5 annual cycles and an exposure of 60-62 GWD/MT. The results can be summarized as follows:

- The solid swelling rate is equivalent to undoped UO_2,
- Thermal conductivity of the doped fuel pellets is equivalent to the undoped fuel in the temperature range up to 1.600°C as determined by instrumented experiments in the OSIRIS test reactor (Muller, 2007),
- Fission gas release of the doped fuel is nearly ½ of the undoped fuel (Table 2-5), due to the precipitation of fission gas bubbles within the large grains and the increased distance required for their diffusion to the grain boundaries and subsequent release (Figure 2-12),
- The doped fuel survived ramp tests in a French *PWR* (CONCERTO Program) to 535 w/cm) at a 335 Δ w/cm under *PWR* conditions and to 480 w/cm at a 230 Δ w/cm under *BWR* conditions with reduced coolant temperature. This was indicated as a significant improvement over undoped UO_2, but no details on the CONCERTO ramp tests were given for the evaluation of the comparison.

Table 2-5: Comparison of Fission Gas Release of Doped and Undoped Fuel After Power Ramp Testing (Delafoy, 2007)

	Ramp terminal level (W/cm)	Fission gas release (%)	
		Non-doped UO_2 fuel	Cr_2O_3-doped fuel
2 cycle ramp tests	460 – 468	16.5	8
(BU ~60 GWd/tU)	530	30*	11
2 cycle ramp tests (BU ~60 GWd/tU)	445	8*	4

* thermo-mechanical calculations

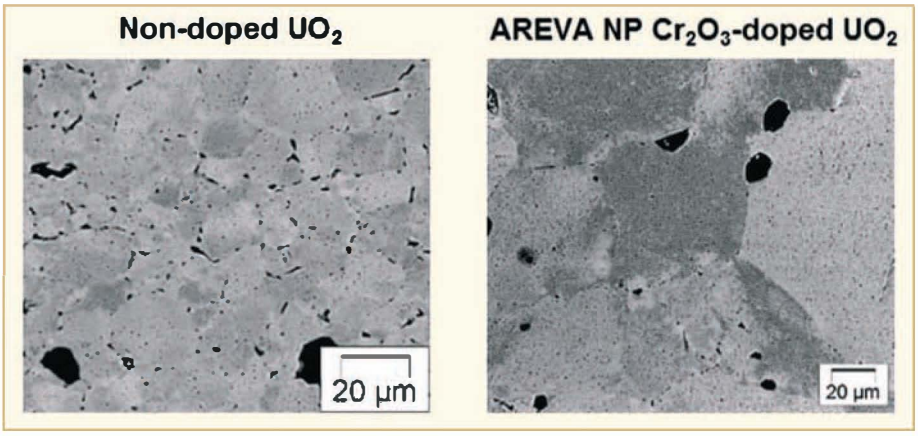

Figure 2-12: Comparison of the Microstructure of Standard UO_2 and Cr_2O_3-Doped Fuels Irradiated to 60 GWD/MT (Delafoy, 2007).

Irradiation of doped fuel is in progress since 2001 in *PWR*s and 2005 in *BWR*s to a target of 70 GWD/MT.

A comparison of UO_2 and Mixed OXide (MOX) fuel, the latter made by two fabrication methods, was made by Japanese irradiations to 72 GWD/MT in the Halden Reactor. The *MOX* fuel was fabricated by the Belgian/French Micronized Master Blend route (*MIMAS*) process and the British Short Binderless Route (*SBR*), their products potentially different in plutonium (Pu) homogeneity. The tests were instrumented with thermocouples and gas pressure measuring devices.

The comparison of peak fuel temperatures did not show significant differences between the three fuel types indicating similar thermal conductivities. The gas pressure was somewhat higher in the *MOX* rods than the UO_2 rods and the *MIMAS* fuel had slightly higher gas release than the *SBR* fuel, Figure 2-13. The latter could be due to somewhat better homogeneity of the *SBR* fuel; however, no conclusions were drawn by the authors except they will investigate this further.

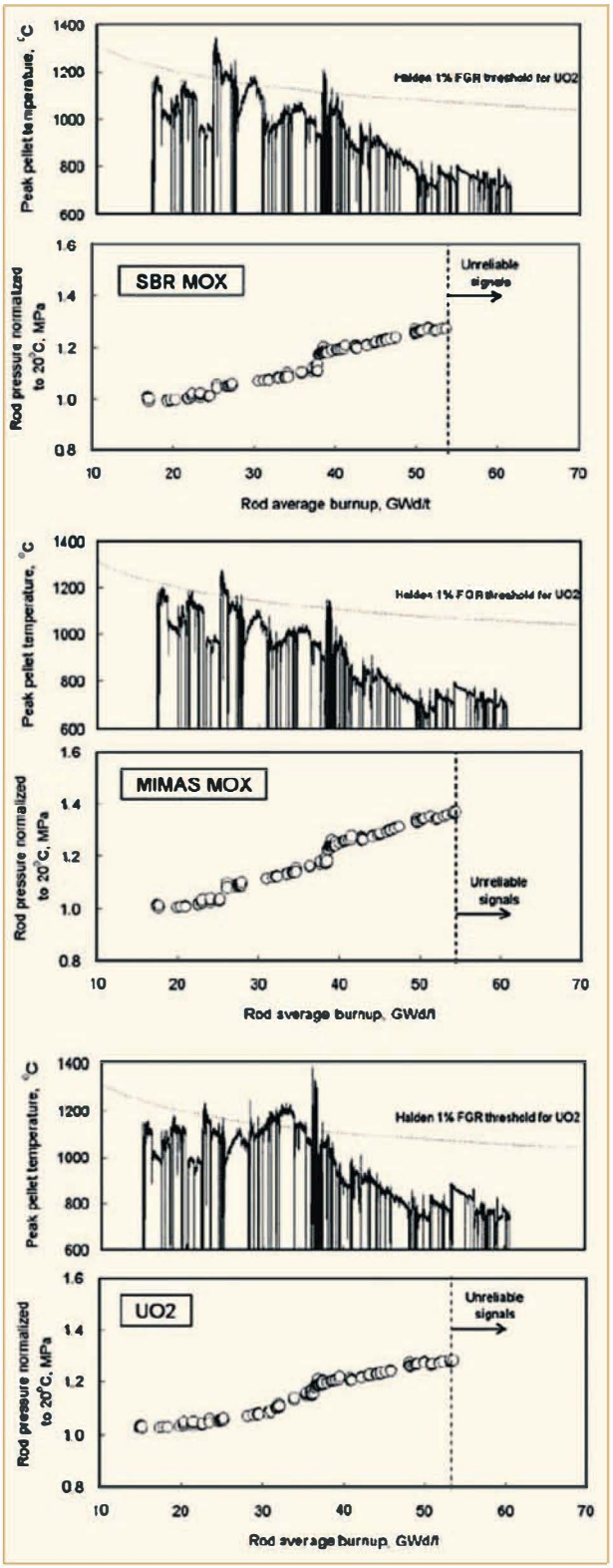

Figure 2-13: Comparison of Normalized Rod Pressure Evolution as a Function of Burnu-up and Fuel Temperature for UO_2 and *MOX* (Fujii, 2007).

The swelling rates of the three fuels, based on stack elongation, were similar and agreed reasonably well with previously measured 0.6% ΔV/V per 10 GWD/MT swelling rate for UO_2. *(Agreement on this UO_2 swelling rate is not universal as noted later.)*

The *high burnup fuel rim structure and properties* of UO_2 and $(U,Gd)_2O_3$ were determined by the irradiation of thin discs 5 mm diameter and 1 mm thick in the Halden reactor. The tests included 4 temperatures and 4 burnup ranges up to 93-104 GWD/MT (Sonoda, 2007). The tests made with 5% $^{16}Gd_2O_3$ and 25% enriched UO_2 are listed in Table 2-6. The rim structure observed on the outer diameter of commercial fuels at high burnup has small sub-grains about 100 nm diameter with small pores of about 1μ. The structures observed in these tests as a function of temperature and burnup show that local restructuring from the original 10μ grain size starts at the 51-53 GWD/MT and is completed at the 75-79 GWD/MT level at the temperatures noted, Figure 2-14. Samples irradiated at high temperatures were not restructured above a level of less than 1.300°C, Figure 2-15. No differences were observed between the urania and gadolinia fuels.

Table 2-6: Burnup and Temperature of UO_2 and (U, Gd)O_2 Samples.

	Rod 1	Rod 2	Rod 3	Rod 4
Stack 1	S11	S21	S31	S41
UO_2 (MWd/kgU)	96	91	90	92
(U,Gd)O_2 (MWd/kgU)	104	93	93	97
Temperature (°C)	530	760	1060	1310
Stack 2	S12	S22	S32	S42
UO_2 (MWd/kgU)	82	73	75	75
(U,Gd)O_2 (MWd/kgU)	84	80	79	84
Temperature (°C)	510	720	1000	1240
Stack 3	S13	S23	S33	S43
UO_2 (MWd/kgU)	55	51	51	51
(U,Gd)O_2 (MWd/kgU)	61	52	53	53
Temperature (°C)	450	660	880	1100
Stack 4	S14	S24	S34	S44
UO_2 (MWd/kgU)	34	34	33	34
(U,Gd)O_2 (MWd/kgU)	33	32	33	34
Temperature (°C)	400	610	770	950

3 Zirconium alloy manufacturing and alloy systems (George Sabol)

3.1 Introduction

In this *ZIRAT12* Report, Manufacturing and Alloy Systems are combined into a single section for two reasons; lack of a sufficient number of new publications in each area for two stand alone sections, and the interdependence of processing variables with the phase relationships for the specific alloys under investigation. The approach to the description of this section is to present an overview of the manufacture of zirconium alloy tubing, sheet, and bar stock, provide general comments on the compositions of Zr-based alloys being developed for *PWR* and *BWR* applications, and then to briefly review the significant aspects of the recent publications on manufacturing and alloy systems. Included in the section are papers on improvements in the economics of manufacturing and quality of products through optimization of organizational structure and materials flow, description of the properties of alternate alloys for *LWR* cladding for high burnup application, and progress in understanding the precipitation and dissolution of hydrides in Zr-based alloys.

3.2 Overview of zirconium alloy manufacturing

The material performance in-reactor is a function of the reactor environment as well as the material microstructure. The microstructure depends on the chemical composition and the manufacturing process of the alloy. Figure 3-1 gives an overview of the manufacture of zirconium alloy strip and tube materials that are used to manufacture fuel cladding, Guide Tubes (*GT*) and grids for *PWR*s, and fuel cladding, water rods, channels and grids for *BWR*s.

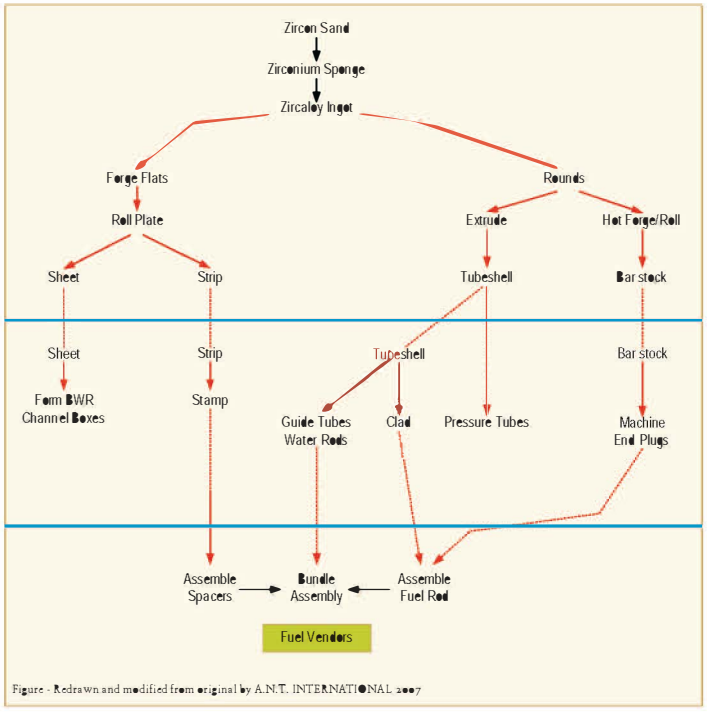

Figure 3-1: Zircaloy Production Outline.

The manufacturing process of different *LWR* zirconium alloy products may be divided into three steps: 1) production of Zr raw material, 2) melting and primary processing (hot deformation), and 3) final product (tube, strip/sheet, bar) fabrication.

Nearly all the zirconium metal is extracted from zircon, Zr-Hf SiO_4, which is found in beach sand, with the richest deposits in Australia. The zirconium to hafnium ratio in zircon is about 50/1, but since Hf has a very large thermal neutron cross section, it is crucial that as much Hf as possible is separated from zirconium during the manufacturing process.

The current dominant process to produce Zr metal is the Kroll process, reduction of zirconium tetrachloride with molten magnesium, which results in zirconium sponge. Zirconium sponge, recycle material from earlier manufacturing, and alloying elements are assembled into an electrode that is arc-melted in a consumable electrode process in a vacuum. The resulting ingot is remelted, usually twice, to increase the homogeneous distribution of the alloying elements.

The ingots are converted to products according to a sequence of plastic deformations to final shape. Deformation processing is divided into hot and cold forming processes. The temperatures in the former are high enough to cause dynamic recrystallization, whereas, the latter processes are done at such a low temperature, usually room temperature, that recrystallization does not occur during deformation. Intermediate recrystallization anneals are performed to restore the ductility after cold deformation.

For round products the ingots are hot forged into round billets, called "logs", by use of a hydraulic press or by rotary forging, the latter giving a more homogeneous plastic deformation. The logs may be further processed directly, or cut into shorter segments for further processing.

The next step in manufacturing is the beta-heat treatment and quenching process. Alloy billets are heated into the high temperature β-phase region (~1100°C) to dissolve the phases formed during the hot working and to homogenize the product by decreasing the microsegregation of the alloying elements. Rapid cooling by water quenching is used to maintain uniformity of alloy distribution by avoiding constitutional segregation as the cooling proceeds through the two-phase (α+β) region and to suppress precipitation of large Second Phase Particles (*SPP*s)

If a "log" was beta-quenched, it is then cut up in smaller sized billets for subsequent processing to tube shells and pressure tubes. Alternately, the "log" may be cut into billets and then β quenched. After the β-quench the solid billets are then pierced to get a central hole (the pierced billet can also be beta-quenched resulting in faster cooling rate). Then the billet with a pierced hole is machined to remove the oxide scale and the surface beneath the oxide that may be contaminated from the earlier processing operations.

For extrusion, the billets are heated to the extrusion temperature (600-750°C), put into the extrusion press, and extruded to tube hollows.

Processing of the extrusions to cladding or guide tubes proceeds in several steps by cold pilgering, also called rocking, or tube reducing. In most cases, three to four reduction passes are required to reduce the extrusion to the final tubing size. After each reduction pass, the tubes must be cleaned and vacuum annealed to prepare them for the next cold reduction pass. The annealing treatments promote recystallization and soften the material. For pressure tubes the extrusions are typically cold drawn to size, with or without an intermediate anneal.

For Zircaloy-2 and -4 used in *BWR*s and *PWR*s the selection of the intermediate annealing temperatures is dictated by the integrated thermal exposure of the material after the β-quench. With increasing thermal exposure, the excess iron, chromium, and nickel (for Zircaloy-2) above the solubility limit are precipitated as second phase intermetallic particles of $Zr(Fe,Cr)_2$ and $Zr_2(Fe,Ni)$. The extent of precipitation and precipitate size increases with thermal exposure. As it has been found that there is a direct relationship between the integrated thermal exposure and corrosion resistance, the thermal exposure is monitored by an "Annealing" parameter, A, which is a measure of the total heat input after the last beta-quenching according to:

$$A = \Sigma t_i \, exp(-Q / RT_i)$$

where t_i (in hours) and T_i (in Kelvin) are the time and temperature of annealing step i
Q is an activation energy, and,
R is the gas constant.

Different activation energies have been used, and values in the range 63,000 to 80,000 cal/mole/K have shown good correlation of thermal exposure with corrosion resistance, Andersson et al., 1987, and Garzarolli et al., 1989. As thermal exposure leads to precipitation and growth of *SPP*s, there is also a relation between the cumulative thermal exposure and particle size, and quantitative relationships have been described by use of a Particle Growth Parameter (*PGP*), Steinberg & Pohlmeyer, 1997, and by a Second Order Cumulative Annealing Parameter (*SOCAP*), Groß & Wadier, 1990. The *PGP* and *SOCAP* relations may offer advantages when accounting for short annealing times, e.g. strips produced by continuous rolling/annealing.

The Zircaloys are usually used in the recrystallized condition in both *PWR*s and *BWR*s. The exception is fuel cladding in *PWR*s, which is used in the Cold Work and Stress Relieved Annealed (*CWSRA*) or partially recrystallized conditions. Use of *RXA* material for grids and guide tubes in *PWR*s is to ensure enough ductility during manufacturing of the fuel assembly structure, which normally involves heavy plastic deformation of the guide tube to interlock it to the spacer grids. *RXA* material also provides reduced irradiation growth and creep compared to material in the *CWSRA* condition, an advantage for dimensional stability of the assembly.

Tubes are straightened after the final anneal. An anneal may be performed after straightening to reduce the residual stresses in the components (introduced during the straightening operation). After the straightening and optional annealing, the oxide scale, surface defects, and surface contamination are removed by pickling and final surface treatment, which typically is a light abrasion. The Inner Diameter (*ID*) of tubing is either flush-pickled or bead blasted to remove surface contamination.

The ingots used for flat products are also forged in the same way as was described for the tubular materials, except that the intermediate form is a slab instead of a 'log". The forged slab may be β-quenched, or hot rolled and β-quenched at a reduced thickness. Beta-quenching of the slab is done at different thicknesses by different manufacturers. Cold rolling commences after cleaning the surface from oxides and conditioning to remove local contamination. The degree of deformation in the individual cold rolling passes is lower than usually applied in pilgering. If continuous rolling and annealing is used, the times at temperature after each cold deformation step are rather low (only a few minutes). Most sheet materials are in the *RXA* condition to get optimum ductility to allow plastic deformation of the sheet into the final product configurations, such as fuel channels and spacer grids, without risk of cracking during subsequent forming operations.

For the Nb-containing alloys, *ZIRLO*™ and M5™, processing of ingots through the β-quench is the same as for the Zircaloys. Subsequent processing, however, is different in that the extrusion and intermediate annealing temperatures are lower for the Nb-containing alloys, Sabol et al., 1989 and 1994, and Gilbon et al., 2000. The β-Zr phase forms at temperatures above 600°C, and this phase is detrimental to corrosion resistance. The *SPP*s in M5 are β-Nb, and those in *ZIRLO* are β-Nb and a $Zr(Nb,Fe)_2$-type phase having a Nb/Fe ratio of ~1.5. Intermediate annealing temperatures for both alloys are typically below 600°C to avoid formation of β-Zr and to prevent excessive growth of the *SPP*s. The average size of the *SPP*s is typically below ~80 nm. The *ZIRLO* and M5 alloys are used as cladding and structural components only in *PWR* fuel assemblies. M5 is used in the *RXA* condition for all applications. *ZIRLO* is used in the *RXA* condition for guide tubes and grids. For fuel cladding *ZIRLO* is used in the *CWSRA* condition, but recently, the "Optimized" version is in the Partially Recrystallized Condition (*PRXA*), Kesterson et al., 2006.

Canadian Deuterium Uranium (*CANDU*) Pressure Tubes are currently fabricated from Zr-2.5%Nb alloy by extrusion in the (α+β) phase field followed by cold working and stress relieving. The fabrication route is summarized in Figure 3-2, Choubey et al., 1996.

4 Mechanical properties (Brian Cox)

There were limited number of results related to mechanical properties published in the past twelve months. Mechanical properties will be covered in greater depth in the *ZIRAT13 AR*.

4.1 *PCI* and *DHC* Cracking Mechanisms

There were no new results published in the past twelve months that shed new light on *PCI* mechanisms. In contrast, there were a number of new papers relevant to Delayed Hydride Cracking (*DHC*) cracking mechanisms. However, three of these were by the same group of authors – Kim et al., 2006 (a, b and c). Two other papers came from *CANDU* authors. A collaboration between Canada, Russia, Sweden and Lithuania to study differences in the behaviour of *CANDU* and *RBMK* Pressure Tubes, Coleman et al., 2007. The international collaborative project compared various properties of the tubes including Velocity. The experimental tubes were prepared by four different routes from the same original electrolytic Zr powder. The four different production routes were:

CW: Cold-worked material similar to *CANDU* tubes.
CW-A: Cold-worked and 540°C annealed tubes similar to *RBMK* tubes.
TMT-1: Material quenched from the (α+β) phase field into water + cold working. Similar to tubes used in Ignalina 1, 1500 *MW-RBMK*.
TMT-2: Similar to ThermoMechanical Treatment (*TMT-1*) but quenched from the (α+β) phase into an argon-helium gas-
mixture. Like material used in Ignalina-2.

DHC cracking velocities for the four different typoes of tubes were measured and results appear to depend on alloy stregth rather than texture and β-Zr phasedistribution. Increases in strength resulting from irradiation also a affected crack growth resistance, except for *TMT-2*.

Cui et al., 2006 have studied the effect of notch-root radii using 15, 30 and 100 μm radius notches. Specimens were given a number of ratcheting cycles where specimens were heated to 270°C to dissolve the hydrogen and then cooled in three steps. Specimens were cycled until failure. Hydride distributions around the notches were affected by the magnitude of the root-radius and the number of cycles to failure increased with root-radious. Failure occurred for all root radii (Figure 4-1) with the highest number of cycles to failure being 184 cycles for a 100 μm radius notch.

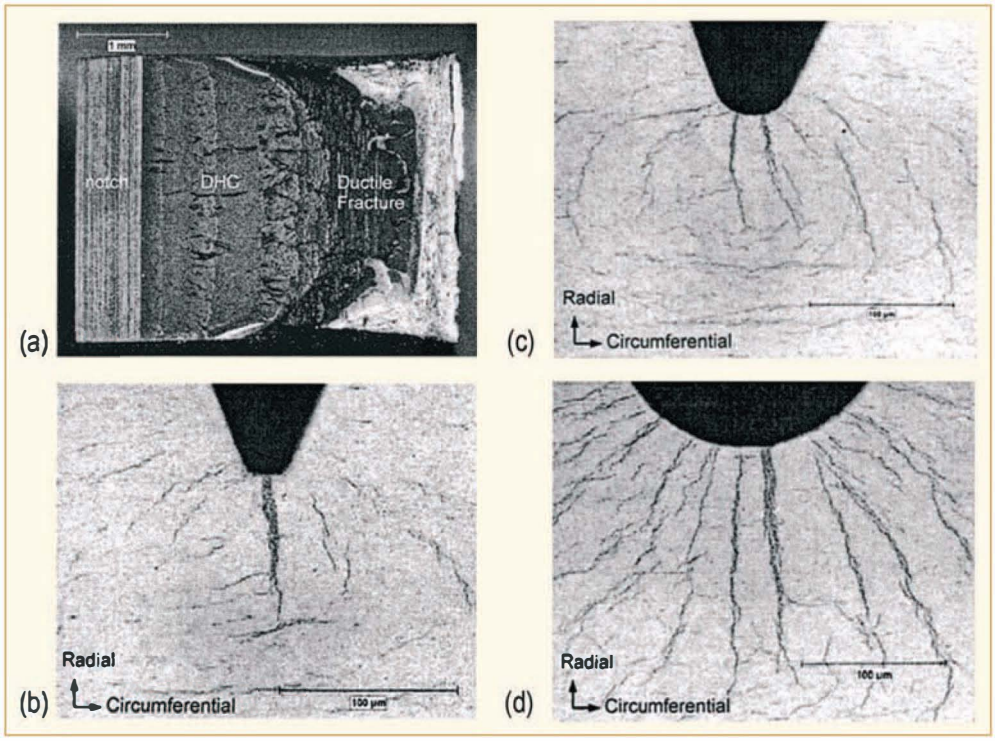

Figure 4-1: (a) Fracture surface of a 30 µm radius sample in test group U-10-4, K_{EFF} = 12 MPa √m, tube B. (Initiated *DHC* in 8th cycle, failed in 11th cycle). (b) Optical micrograph of flaw-tip hydrides in a 15 µm radius sample in test group U-8-2, K_{EFF} = 8 MPa √m, 114 cycles. (c) Optical micrograph of flaw-tip hydrides in a 3 µm radius sample in test group U-10-1, K_{EFF} = 8 MPa √m, 117 cycles. (d) Optical micrograph of flaw-tip hydrides in a 10 µm radius sample in test group U-12-1, K_{EFF} = 12 MPa √m, 184 cycles.

The basis of the *DHC* process is that hydrogen in solution in tetra-hedral sites dilates the Zr lattice. Thus, dilating the Zr lattice mechanically by TRIAXIAL stress causes H or D to migrate into the dilated region of the lattice. H/D will continue to migrate into the dilated lattice until the terminal solid solubility is reached (*TSS*) when hydride precipitates at the notch.

Because the partial mola volumes of hydrogen in solution in Zr and hydrogen precipitated as hydride in Zr are essentially identical at ~300°C, Mac Ewen et al, 1985. This precipitation does not affect the local stress distribution. Thus it is the lattice dilation by a triaxial stress that is critical in initiating *DHC*, biaxial stresses are not effective.

Kim et al, 2006 (a, b and c) do not accept that significant amount of hydrogen will diffuse to the crack tip with triaxial stressing and instead conclude that supersaturation of hydrogen locally as a result of approaching the cracking temperature by cooling from above combined with local stressing from the S-hydride to γ-hydride transformation. However, a volume change due to the S→γ phase change is not well established and further studies are needed.

5 Dimension stability (Ron Adamson)

5.1 Introduction

One of the most unique aspects of material behavior in a nuclear power plant is the effect of radiation (mainly neutrons) on the dimensional stability of reactor components. In fast breeder reactors the Fe and Ni-based alloys creep and swell; that is, they change dimensions in response to a stress and change their volume in response to radiation damage. In light water reactors, zirconium alloy structural components do not swell, but do change their dimensions through radiation creep and the approximately constant volume process called irradiation growth. Radiation effects are not unexpected since during the lifetime of a typical component every atom is displaced from its normal lattice position at least 20 times. With the possible exception of elastic properties like Young's Modulus, the properties needed for reliable fuel assembly performance are affected by irradiation. A straightforward summary of such effects is given by Adamson & Cox, 2005 **and** Adamson, 2000

Practical effects of dimensional instabilities are well known and it is rare that a technical conference in the reactor performance field does not include discussions on the topic. Because of the difference in pressure inside and outside the fuel rod, cladding creeps down on the fuel early in life, and then creeps out again later in life as the fuel begins to swell. A major issue is to have creep strength sufficient to resist outward movement of the cladding if fission gas pressure becomes high at high burnups. *PWR* guide tubes can creep downward or laterally due to forces imposed by fuel assembly hold down forces or cross flow hydraulic forces – both leading to assembly bow which can interfere with smooth control rod motion. *BWR* channels can creep out or budge in response to differential water pressures across the channel wall, again leading toward control blade interference. Fuel rods, water rods or boxes, guide tubes, and tie rods can lengthen, possibly leading to bowing problems. (For calibration, a recrystallized (*RX* or *RXA*) Zircaloy water rod or guide tube could lengthen due to irradiation growth more than 2 cm. during service; a cold worked/stress relieved (*SRA*) component could lengthen more than 6 cm.) Even *RX* spacer/grids could widen enough due to irradiation growth (if texture or heat treatment was not optimized) to cause uncomfortable interference with the channel. And channels and guide tubes can bow due to uneven length changes on opposite sides of the structure.

In addition, corrosion leading to hydrogen absorption in Zircaloy can contribute to component dimensional instability due, at least in part, to the fact that the volume of zirconium hydride is about 16% larger than zirconium. The above discussion leads to the concept that understanding the mechanisms of dimensional instability in the aggressive environment of the nuclear core is important for more than just academic reasons. Reliability of materials and structure performance can depend on such understanding.

A comprehensive review of dimensional stability has been given in the *ZIRAT7* Special Topical Report – "Dimensional Stability of Zirconium Alloys"; Adamson & Rudling, 2002. The sources of dimensional changes of reactor components (in addition to changes caused by conventional thermal expansion and contraction) are: irradiation growth, irradiation creep, thermal creep, stress relaxation (which is a combination of thermal and irradiation creep), and hydrogen and hydride formation.

Irradiation effects are primarily related to the flow of irradiation-produced point defects to sinks such as grain boundaries, deformation-produced dislocations, irradiation produced dislocation loops, and alloying and impurity element complexes. In zirconium alloys, crystallographic and diffusional anisotropy are key elements in producing dimensional changes.

5 Dimension stability (Ron Adamson)

5.1 Introduction

One of the most unique aspects of material behavior in a nuclear power plant is the effect of radiation (mainly neutrons) on the dimensional stability of reactor components. In fast breeder reactors the Fe and Ni-based alloys creep and swell; that is, they change dimensions in response to a stress and change their volume in response to radiation damage. In light water reactors, zirconium alloy structural components do not swell, but do change their dimensions through radiation creep and the approximately constant volume process called irradiation growth. Radiation effects are not unexpected since during the lifetime of a typical component every atom is displaced from its normal lattice position at least 20 times. With the possible exception of elastic properties like Young's Modulus, the properties needed for reliable fuel assembly performance are affected by irradiation. A straightforward summary of such effects is given by Adamson & Cox, 2005 **and** Adamson, 2000

Practical effects of dimensional instabilities are well known and it is rare that a technical conference in the reactor performance field does not include discussions on the topic. Because of the difference in pressure inside and outside the fuel rod, cladding creeps down on the fuel early in life, and then creeps out again later in life as the fuel begins to swell. A major issue is to have creep strength sufficient to resist outward movement of the cladding if fission gas pressure becomes high at high burnups. *PWR* guide tubes can creep downward or laterally due to forces imposed by fuel assembly hold down forces or cross flow hydraulic forces – both leading to assembly bow which can interfere with smooth control rod motion. *BWR* channels can creep out or budge in response to differential water pressures across the channel wall, again leading toward control blade interference. Fuel rods, water rods or boxes, guide tubes, and tie rods can lengthen, possibly leading to bowing problems. (For calibration, a recrystallized (*RX* or *RXA*) Zircaloy water rod or guide tube could lengthen due to irradiation growth more than 2 cm. during service; a cold worked/stress relieved (*SRA*) component could lengthen more than 6 cm.) Even *RX* spacer/grids could widen enough due to irradiation growth (if texture or heat treatment was not optimized) to cause uncomfortable interference with the channel. And channels and guide tubes can bow due to uneven length changes on opposite sides of the structure.

In addition, corrosion leading to hydrogen absorption in Zircaloy can contribute to component dimensional instability due, at least in part, to the fact that the volume of zirconium hydride is about 16% larger than zirconium. The above discussion leads to the concept that understanding the mechanisms of dimensional instability in the aggressive environment of the nuclear core is important for more than just academic reasons. Reliability of materials and structure performance can depend on such understanding.

A comprehensive review of dimensional stability has been given in the *ZIRAT7* Special Topical Report – "Dimensional Stability of Zirconium Alloys"; Adamson & Rudling, 2002. The sources of dimensional changes of reactor components (in addition to changes caused by conventional thermal expansion and contraction) are: irradiation growth, irradiation creep, thermal creep, stress relaxation (which is a combination of thermal and irradiation creep), and hydrogen and hydride formation.

Irradiation effects are primarily related to the flow of irradiation-produced point defects to sinks such as grain boundaries, deformation-produced dislocations, irradiation produced dislocation loops, and alloying and impurity element complexes. In zirconium alloys, crystallographic and diffusional anisotropy are key elements in producing dimensional changes.

In the past, hydrogen effects have been considered to be additive to and independent of irradiation; however, recent data have brought this assumption into question. It is certain that corrosion-produced hydrogen does cause significant dimensional changes simply due to the 16-17% difference in density between zirconium hydride and zirconium. A length change of on the order of 0.25% can be induced by 1000 ppm hydrogen in an unirradiated material. Whether or not the presence of hydrides and/or hydrogen contributes to the mechanisms of irradiation creep and growth is yet to be determined.

Fuel rod diametral changes are caused by stress dependent creep processes. Fuel rod length changes are caused by several phenomena:

- Stress free axial elongation due to irradiation growth.
- Anisotropic creep (before pellet/cladding contact) due to external reactor system pressure. Because of the tubing texture, axial elongation results from creep down of the cladding diameter; however for heavily cold worked material, it has been reported that some shrinkage may occur. In a non-textured material such as stainless steel, creep down of the cladding would only result in an increase in cladding thickness, with no change in length.
- Creep due to Pellet Cladding Mechanical Interaction (*PCMI*) after hard contact between the cladding and fuel. This occurs in mid-life, depending on the cladding creep properties and the stability of the fuel.
- Hydriding of the cladding due to corrosion.

Bow of a component such as a *BWR* channel or *PWR* control rod assembly can occur if one side of the component changes length more than the other side. Such differential length changes occur due to differential stress and creep, relaxation of differential residual stresses, or differential growth due to differences in flux-induced fluence, texture, material cold work, and hydrogen content (and, although not usually present, differences in temperature or alloying content.

Review of the mid-2005 through late 2006 literature on dimensional stability was reported in the *ZIRAT11 AR*, Adamson et al., 2006. Reported highlights included:

- The book Zirconium in the Nuclear Industry, 14th International Symposium, *ASTM* STP 1467, Peter Rudling and Bruce Kammenzind, editors, *ASTM* International, West Conshohocken, PA, 2005, was issued in 2006. It contains the final version of papers presented at the Stockholm meeting of June 2004. Most of the papers were reviewed in the *ZIRAT10 AR*, so just brief comments were given to allow the reader to easily look up the papers in the book.
- A review was given on the effect of temperature on growth. This is related to understanding differences between irradiation growth of Zircaloy published in different studies.
- *GNF*-Ziron (Zr1.46%Sn.26%Fe.10%Cr.05%Ni) and High Fe-Ni (Zr1.43%Sn.26Fe.10Ni) are being introduced as alloys to resist corrosion and hydriding at high burnup. These alloys are reported as having irradiation growth properties very similar to and irradiation creep strength slightly higher than standard Zircaloy.
- The standard version of *ZIRLO*, Zr1Nb1Sn.1Fe, has been optimized by Westinghouse to Zr1Nb.7Sn.1Fe in order to increase corrosion resistance. The standard *ZIRLO* has a cold-worked-stress-relieved (*SRA*) microstructure while Optimized *ZIRLO* has a "low degree of Partial Recrystallization (*PRX*)" microstructure. For one cycle of irradiation, irradiation growth and creep are reported to be very similar to the standard *ZIRLO*.
- Previous *ZIRAT*/Information on Zirconium Alloys (*IZNA*) *AR*s have noted with interest the difference in growth behavior between E110 and M5, both nominally Zr1Nb alloys. E110 has consistently exhibited accelerated breakaway growth while M5 has not. In the past E110 has been made from a relatively pure electrolytic powder blended with zirconium iodide while M5 is made from Kroll process sponge zirconium. New data on E110 growth as affected by the zirconium source was presented. E110 made from sponge Zr has irradiation growth behavior similar to that of M5. Minor impurities, oxygen, silicon and iron apparently have a significant effect on growth.

- New experimental work on irradiation creep mechanisms of Zr2.5%Nb was presented. Creep deformation did not follow the irradiation damage or fluence profiles, but did roughly follow the profile of Nb content of the alpha-Zr grains. Since the latter is strongly temperature-dependent as well as irradiation-dependent, both need to be accounted for when predicting pressure tube creep.
- Extensive hot cell examination data for the pressurized water *VVER* Zr1%Nb fuel bundle components were reported. Cladding creepdown and fuel swelling produced standard dimensional change effects.

The current *ZIRAT12 AR* reviews the literature from late 2006 to late 2007.

5.2 Effect of oxide-induced stresses

The Westinghouse work of Kesterson et al., 2000 and King et al., 2002 on unusual elongation of guide tubes and grids has been reported many times in the *ZIRAT/IZNA AR*s. A significant increment in strain is due to volume expansion of hydrides, but some unexplained strain remains. Westinghouse recognized that oxide stresses could be important, but did not have firm data to quantify the effect. Strain as a function of oxide thickness and of hydrogen content is given in Figure 5-1. It is seen that the strain profiles correspond to both oxide thickness and hydrogen profiles. Figure 5-2 shows laboratory data on unirradiated material exposed to 366°C (589K) water containing 700 ppm lithium. For Zircaloy-4 thin strips consistently had more "growth" than thick strips, indicating a possible effect of oxide-induced stress; however Zirlo material (somewhat stronger than Zircaloy) showed no influence of oxide.

6 Corrosion and hydriding

6.1 Out-reactor corrosion and hydriding (Brian Cox)

The past year has presented some interesting new work, especially at the 15th *ASTM* Symposium on Zr in the Nuclear Industry. In addition results from an earlier conference – the 2005 Water Reactor Fuel Performance Meeting in Kyoto, Japan, Oct 2-6th have been reissued as the Sept. 2006 Special Issue of the Journal of Nuclear Science and Technology. Some rewriting of the conference papers was requested because of space limitations in the Journal, but in most instances the figures and data remain exactly the same as at the Kyoto Conference. Although nominally the Sept 2006 edition of the journal, receipt of the journal was delayed to December. The papers containing significant out-reactor corrosion information were the following: Jeong et al., 2006 "Out-of-Pile and In-Pile Performance of Advanced Zirconium Alloys (*HANA*) for High Burn-up Fuel". The figures are exactly the same as at the Kyoto Conference and were reported in the *ZIRAT11 AR* (Section 7.1, pp 7-14 to 7-18). The text was revised and condensed, but without any change in the conclusions. Takeda et al., 2006 "Effect of Metallographic Factor on Hydrogen Pickup Properties of Zircaloy-2". Again, the results were the same as those presented in Kyoto and with the exception of the supercritical steam tests, differences between the alloys were small. Since no error bars were presented and no indication of the multiplicity of the specimens was provided, it is difficult to say whether or not the small differeces in corrosion were statistically significant. Since no Fresnel Contrast was used in their *TEM* studies it is impossible to distinguish between *H/D* diffusion through the ZrO_2 lattice and migration through physical flaws in the oxide. Papers relevant to in-reactor behaviour are covered in Section 6.1.1.

Park et al., 2006 present data on the corrosion behaviour and oxide properties of the *HANA-6* alloy (Zr-1.1% Nb-0.05% Cu). The corrosion data are essentially the same as those presented previously; as are the *TEM* micrographs of *SPPs*, Figure 6-1. However, some new microscope studies showing a lack of layering in the oxide films, Figure 6-2, and the presence of Cu in both the β-Nb and ZrNbFe *SPPs* were added. Lower nanohardness of the oxide, when compared to similar micrographs of oxide on Zircaloy-4 were presented, Figure 6-3. Distinct cracks were observed in the oxide formed on Zircaloy-4; but not in that formed on *HANA-6*. However, since Fresnel Contrast was not used, it is possible a through-focus series would show that some of the "black lines" on the *HANA-6* oxide micrograph might prove to be fine cracks, Figure 6-4.

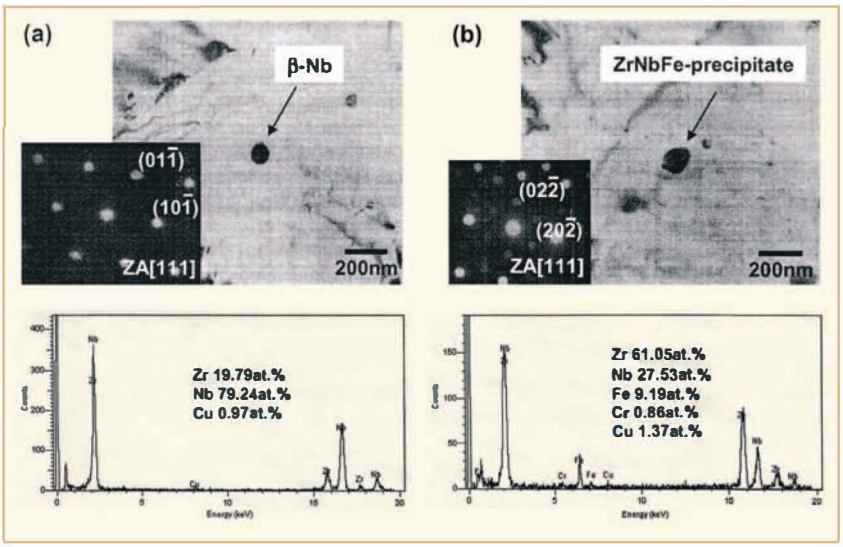

Figure 6-1: *TEM* bright field image, selected area diffraction pattern and *EDS* spectrum with the analyzed chemical composition for the β-Nb and ZrNbFe-precipitate in ZrNbCu annealed at 470°C.

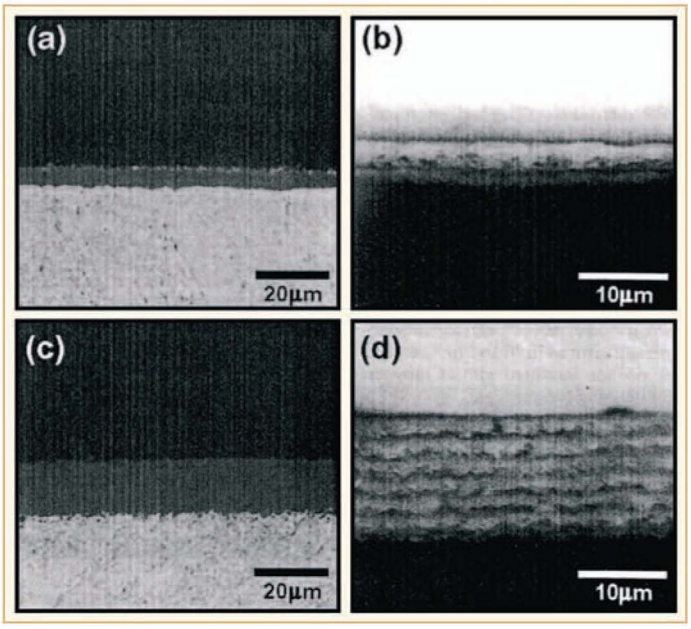

Figure 6-2: (a) and (c) reflected and (b) and (d) transmitted light optical micrographs on the cross-section of the oxide formed on the (a) and (b) ZrNbCu annealed at 470°C for 8 h and (c) and (d) Zircaloy-4 after a corrosion test for 1000 days in the *PWR*-simulating loop conditions.

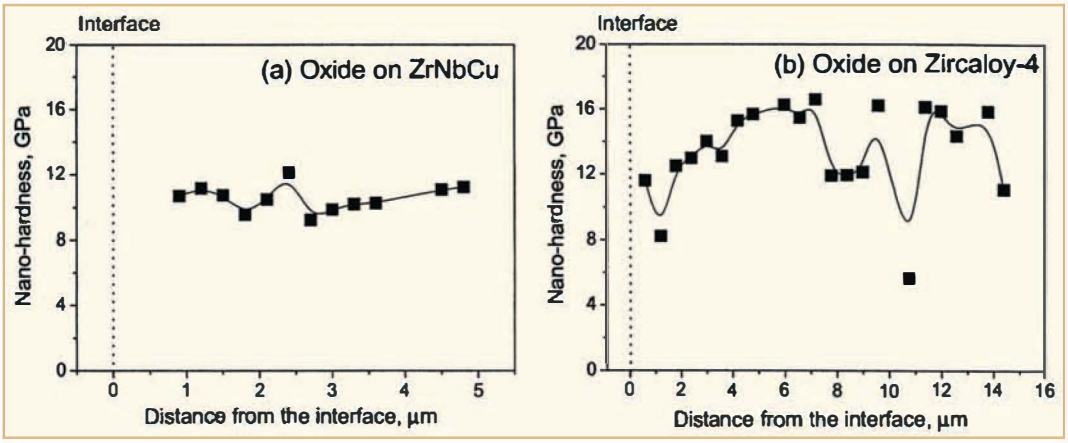

Figure 6-3: Nano-hardness as a function of the distance from the interface in the oxide formed (a) ZrNbCu annealed at 470°C for 8 h and (b) Zircaloy-4 after a corrosion test for 1000 days in the *PWR*-simulating loop condition.

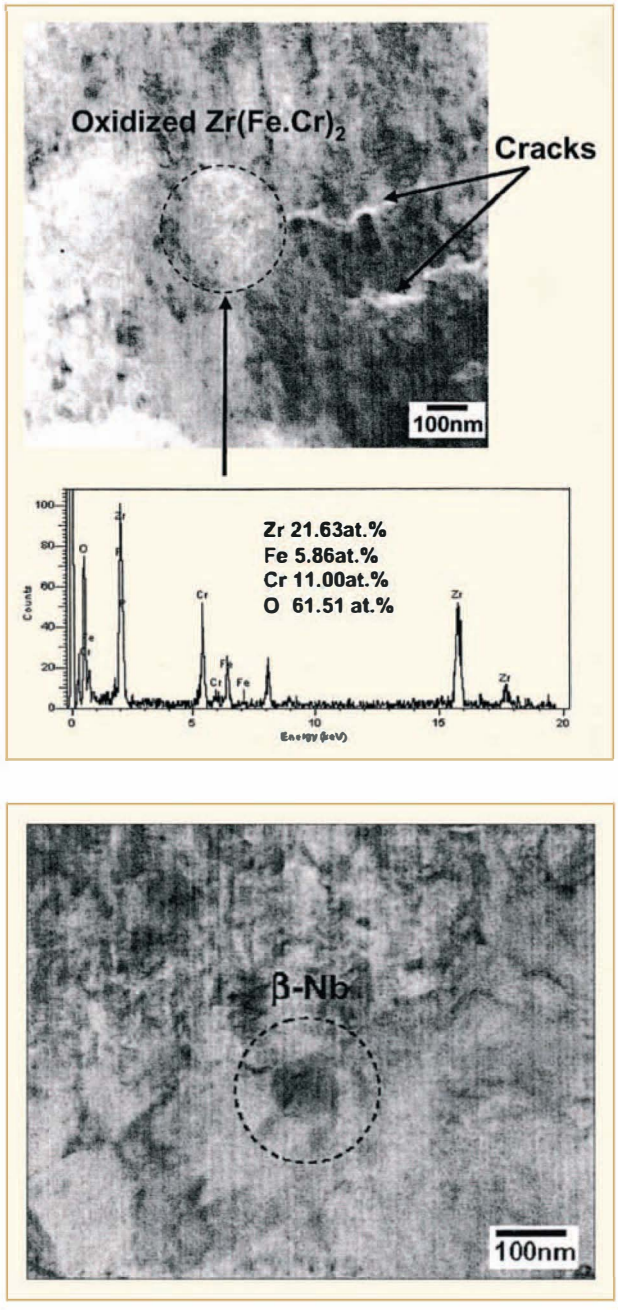

Figure 6-4: (a) Zr(Fe, Cr)2 precipitate in the oxide formed on Zircaloy-4 corroded to 1000 days in the *PWR*-simulating loop condition. (b) β-Nb in the oxide formed on ZrNbCu corroded to 1000 days in the *PWR*-simulating loop condition.

7 Primary failure and secondary degradation (Peter Rudling)

There were limited number of results related to primary failure and secondary degradation published in the open literature. The utility proprietary information, that has been cleared by the respecitve utility for publication in the *ZIRAT* Program, are provided in Appendix A.

8 Cladding performance under accident conditions (Alfred Strasser)

8.1 Loss-of-coolant accident (*LOCA*)

8.1.1 Introduction

The design basis *LOCA* is the double-ended, or guillotine, break of one of the cold, main coolant pipes of a *PWR* or one of the intake pipes to the recirculation pump of a *BWR*.

The *LOCA* process starts by the decrease and ultimate loss of coolant flow at the same time that the reactor is depressurized, Figure 8-1. The loss of coolant flow decreases heat transfer from the fuel, increases the fuel temperature and causes a significant temperature rise of the cladding. The decrease in system pressure causes a pressure drop across and a hoop stress in the cladding. The result is the plastic deformation, or *ballooning* of the cladding. The extent of the ballooning is dependant on:

- Creep strength of the cladding.
- Stress in the cladding and the corresponding strain rate.
- Temperature and the rate of temperature increase.

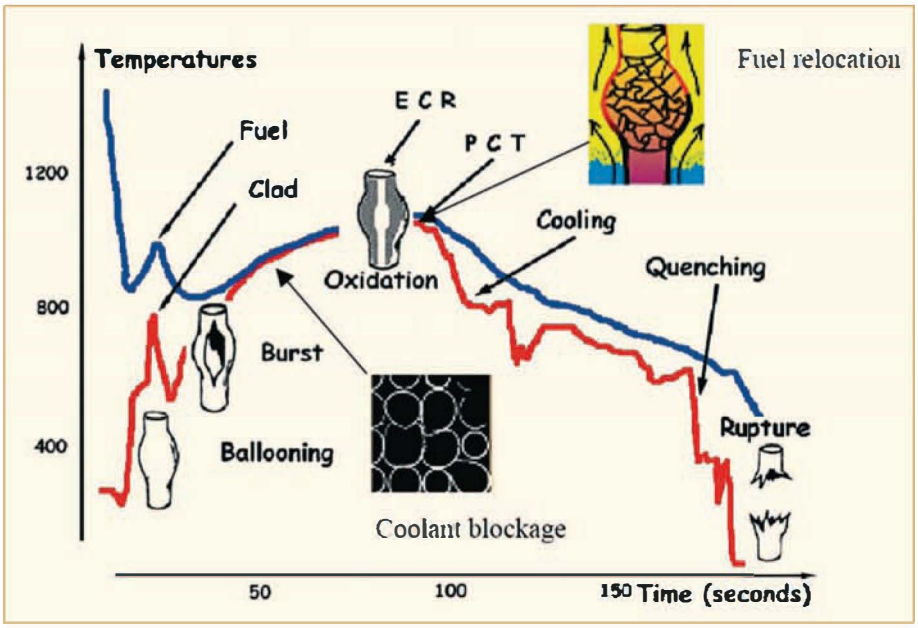

Figure 8-1: Typical *LOCA* in a *PWR*.

Depending on the temperature, the cladding ductility and the rod internal pressure, the cladding will either stay intact or may burst. Ballooning of the cladding can result in coolant blockage and reduce fuel coolability. The main objective of the *LOCA* criteria established by the regulators is to maintain core coolability.

The increasing temperatures and steam will cause the intact cladding to *oxidize* on the *OD* and the burst cladding to oxidize on both the *OD* and *ID* (*two sided oxidation*) until the Emergency Core Cooling System (*ECCS*) is activated and the water quenches the cladding. The oxidation at the high *LOCA* temperatures will increase the oxygen and hydrogen content in the cladding, reducing its ductility and resistance to rupture. The process and final structure of the cladding after a *LOCA* cycle is shown on Figure 8-2:

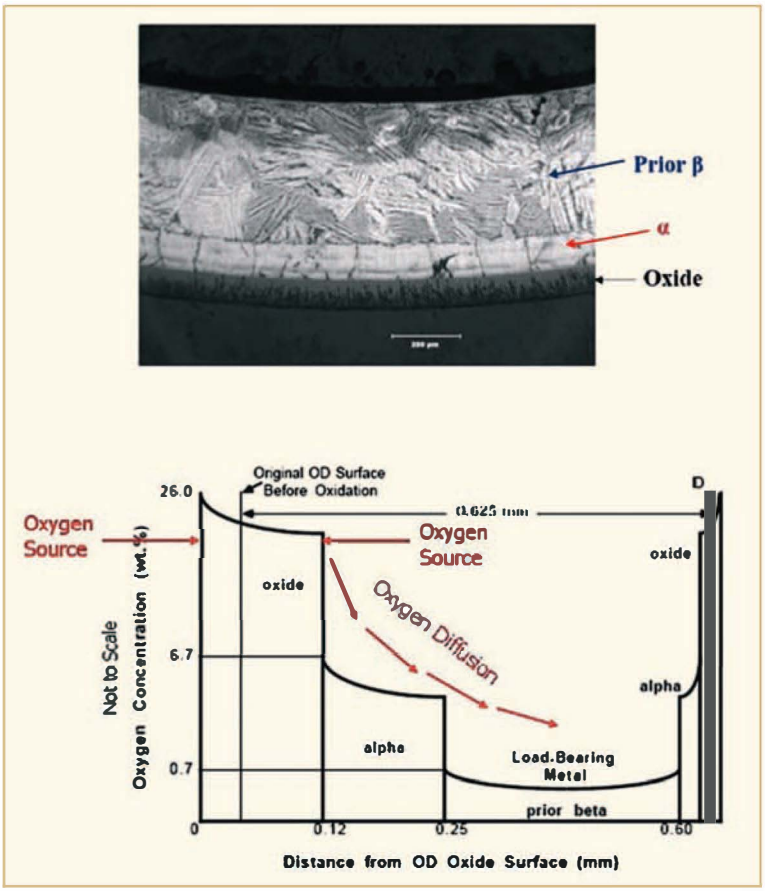

Figure 8-2: Structure of oxidized cladding, Meyer & Billone, 2005.

- First, the high water and steam temperatures increase their reaction rates with the cladding and increase the conversion of the cladding surface into thicker ZrO_2 films.
- As the *LOCA* temperature passes the levels where α→β transformations start and finish, shown in Figure 8-3 for Zircaloy 4 and M5, the resulting structure consists of:
  - the growing ZrO2 layer,
  - a brittle zirconium alloy layer with a very high oxygen content which stabilizes the α phase, formed by diffusion of oxygen from the oxide layer,
  - the bulk cladding which is now in the β phase, has a high solubility for hydrogen.; the hydrogen picked up by the cladding from the water-metal reaction increases the solubility of oxygen in the β layer.

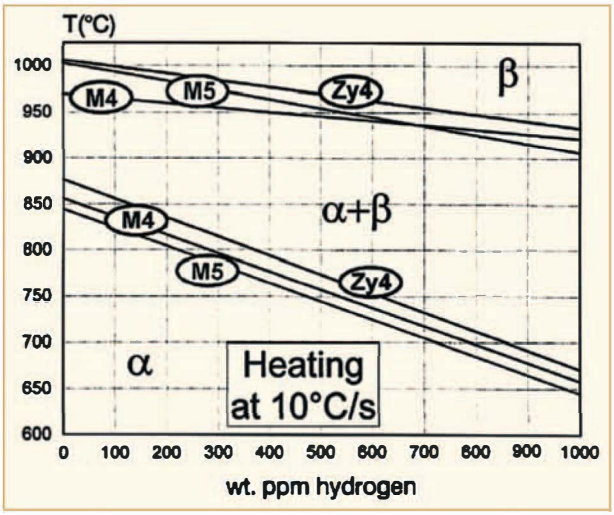

Figure 8-3: The α/β phase transformation temperatures of Zry-4, M4 and M5 alloys as a function of the hydrogen content for a heating rate of 10°C/s, Brachet et al., 2002.

- The ZrO_2 and oxygen stabilized α layers grow with continued diffusion of oxygen and hydrogen from the water reaction. The increasing amount of oxygen convert some of the β phase to oxygen stabilized α phase with the concurrent shrinkage of the β phase. The remaining β phase cladding wall thickness is transformed to α phase, or "prior β phase", on cooling and is the only stsructural part of the cladding that can insure its integrity.

The sources and role of hydrogen in the embrittlement of the cladding includes hydrogen from the corrosion reaction during normal operation and hydrogen from the reaction with the *LOCA* steam. In addition hydrogen increases the solubility of oxygen in the β phase at high temperatures and oxygen, in combination with hydrogen, are then the two major elements that cause cladding embrittlement by the growth of the α layer and the shrinkage of the structural, prior β layer.

Integrity of the cladding is based on the properties of the former β zone, since the ZrO_2 and oxygen stabilized α zones are too brittle to sustain a load. The embrittlement criteria are based on properties of the prior β layer measured on post-simulated *LOCA* tests of unirradiated Zircaloy-4, by ring compression tests (Hobson & Rittenhouse, 1972) and related to oxidation, or Equivalent Cladding Reacted (*ECR*), calculated by the Baker-Just equation. It should be noted that the oxide thickness of the samples were never actually measured during those tests, so that the current *ECR* criteria depend on their relationship to the use of the Baker-Just equation. Modification of this relationship by revised criteria are under discussion with the regulators.

Since the mechanical properties of the prior β zone could change as a function of extended burnup and increased oxygen and hydrogen contents, the *NRC* is evaluating the effects on its properties and the potential need for changing the criteria. Their objective is to make the *LOCA* criteria material independent, and perhaps independent of *%ECR* while maintaining the peak cladding temperature as discussed subsequently.

The entrance of the *emergency coolant will quench and cool* the cladding temperature and the cladding then may rupture due to thermal stresses, or differential expansion of fuel assembly components, in the event the cladding ductility is insufficient to accommodate the strain. The cladding temperature will be reduced at a rapid rate (1° – 5°C/sec) by re-wetting the cladding heat transfer surface. The process will collapse the vapor film on the cladding *OD* and cooling will be by nucleate boiling. Thermal shock due to the sudden change in heat transfer conditions can fracture the cladding at this stage and the ability of the cladding to withstand the thermal stresses will depend on the extent of oxidation that occurred during the *LOCA* transient. Since, however, all the hydrogen is likely to be in solution at these temperatures, hydrogen is unlikely to contribute to the embrittlement except to the extent that its presence increased the oxygen solubility and the increased oxygen content in turn increased the embrittled condition of the cladding.

9 Fuel related issues during intermediate storage and transportation

There were limited number of results related to fuel performance during intermediate storage and transportation published in the past twelve months. This topic will be covered in greater depth in the *ZIRAT13 AR*.

10 Potential burnup limitations

10.1 Introduction

The potential fuel assembly burnup limitations related to zirconium alloy components are summarized in this Section. The burnup limitation that have actually been reached, but have been or are being extended, are:

- Corrosion limits of Zry-4 in high power *PWR*s, are extended by the alternate use of improved cladding alloys. Improved corrosion performance by the new alloys may allow the utilities to use the added margins, to modify plant operation e.g., to lower fuel cycle cost. However, this modified operation will in most cases result in higher corrosion duty of the zirconium materials. Thus, it is believed that the corrosion may always be limiting for plant operation even with the new type of alloys. Furthermore, the influence of *CRUD* on corrosion may increase with increasing duty.
- Bowing of *PWR* fuel assemblies contributed in part by irradiation growth, creep and hydriding of Zry-4, has been reduced by improved guide tube materials (i.e., lower irradiation growth and hydriding rates), reduced assembly holddown forces, and other mechanical/themomechanical design changes, but not yet finally eliminated.
- Bowing of *BWR* channels, extended by improved manufacturing processes, design changes such as variable wall channel thickness with relatively thicker corners, and in-core channel management programs.
- *RIA* and *LOCA* related burnup licensing limits are in the process of being assessed by additional experimental data and analyses. It would appear that the current *LOCA* limits are sufficiently conservative for fuel burnups up to 75 MWd/kgU. The *RIA* limits (threshold enthalpies) may continue to decrease as a function of burnup due to the increase in clad corrosion and hydrogen uptake.
- The categories of event likely to eventually limit reliably and safely achievable burnup levels are outlined below. The zirconium alloy component most sensitive to the limits and potential methods for extending the limits are noted below.

10.2 Corrosion and mechancial properties related to oxide thickness and H pickup

- *BWR*s: increased uniform and shadow corrosion, oxide thickness spalling, increased hydrogen pickup, and formation of radial hydrides due to longer residence time, higher power, modern power histories, and water chemistry changes. Current crucial issues are: shadow corrosion mechanisms its effect on channel bow, late increased corrosion and hydrogen pickup of Zry-2 at high burnups, and formation of radial hydrides, *CRUD*-chemistry-corrosion interaction, effect of water chemistry impurities, as well as specific effects of *NMCA* with or without Zn-injection.
- *PWR*s: increased uniform corrosion, oxide thickness, spalling, and new Zr alloys due to longer residence time and higher Li, higher power, more boiling. The development of new Zr-alloys is still ongoing. The data base for several of the new alloys is still limited. Zr-Nb alloys are occasionally affected by accelerated corrosion due to surface contaminations and/or boiling. Welding of the new alloys may need improved processes (Zr-Nb alloys) and chemical compositions between dissimilar metals such as e.g. *ZIRLO* and Zry-4 may result in inferior corrosion resistance. Luckily, the corrosion temperatures at these elevations in the core are significantly lower than the peak temperatures.
- Decreased ductility and fracture toughness as consequence of the increased hydrogen pickup during any situation (e.g., *RIA*, *PCMI*, *LOCA* and post-*LOCA* events, seismic event, transport container drop-accident conditions).

- Increased growth due to higher hydride volume and thick oxide layers.
- Increased corrosion due to impact of hydrides at the cladding outer surface.
- Impact of corrosion and hydrogen pickup on creep behaviour of fuel claddings during class 1-IV events and during intermediate storage.
- Increased effects of irradiation and hydrides on the fracture toughness of thin-walled zirconium alloy components.

Most sensitive component

Spacer and fuel claddings.

Increase margin for *PWR*

- Improved knowledge of corrosion and hydrogen pickup mechanisms.
- Improved alloys with appropriate fabrication processes: *ZIRLO*, *MDA*, *NDA*, and M5/Zr1Nb. Duplex is another alternative that may be necessary to achieve satisfactory mechanical properties.
- Zr-alloys such as Optimised *ZIRLO*, Modified *MDA*, S2, Modified E635 with reduced Sn content in comparison to the original composition of *ZIRLO*, *MDA*, *NDA* and E635 are being explored.
- Change to enriched **B** soluble shim to reduce Li. There is however a fear that enriched **B** would increase *AOA* potential, i.e., more absorption per g. **B**, even though there may be less **B**.
- Improved water chemistry and *CRUD* control.
- Increase corrosion resistance of steam generator materials.

Increase margin for *BWR*

- Improved knowledge of corrosion and hydrogen pickup mechanisms at high burnups.
- Modification of manufacturing processes (to get optimum sized, more stable second phase particles).
- Zry-4 fuel channels for controlled positions
- Improved alloys under development.

Improved water chemistry and *CRUD* control.

10.3 Dimensional stability

- Increased dimensional changes of components and differential dimensional changes between them resulting in reduced fuel rod spacing or even rod contact, guide tube bowing, fuel assembly bowing, spacer cell and envelope dimensions, *BWR* fuel channel and *PWR* fuel assembly bow may result in:
  - decreased thermal margins (*LOCA* and dry-out)
  - control rod insertion difficulties (safety issue)

Most sensitive component

Potentially all zirconium alloy components, but currently *PWR* guide tubes and *BWR* channels. Also *BWR* spacers have occasionally increased so much in dimensions that unloading of the assembly from the outer channel was very difficult.

Increase margin for *PWR*

- Alloys with lower growth and hydriding rates for guide tubes – *ZIRLO*, M5, E635 (Anikuloy).
- Modified mechanical design to provide lower hold-down forces, stiffer assemblies, etc.
- Beta-quenched material after the last plastic deformation step during manufacturing. (Beta-quenched materials do normally, however, show higher corrosion rate and lower ductility. These properties might be improved by an appropriate final heat-treatment in the alpha-phase. Also applies o *BWR* materials).

Increase margin for *BWR*

- Uniform microstructure and texture throughout the flow channel.
- Use of lower growth material, such as beta-quenched material in as-fabricated step, NSF or other Nb-modified zirconium alloys.
- Channel management programs, including assessment of degree of control over specific reactor periods.
- More corrosion and shadow-corrosion resistant material in channels and spacers.
- Increased understanding of basic phenomena driving the channel bow process, including flux and hydrogen-driven processes.
- Lowered hydride pickup and increased uniformity of hydride distribution in channels and spacers through heat treatment and alloy choice.

10.4 *PCI* in *BWR*s and *PWR*S

Increased sensitivity for *PCI/PCMI* due to:

- More fission products (I, Cs and Cd) produced.
- Increased Transient Fission Gas Release, *TFGR*.
- Formation of a rim zone at the pellet periphery at fuel pellet average burnup of about 50 MWd/kgU.
- Fuel-clad bonding at fuel pellet average burnup of about 50 MWd/kgU.
- Increased swelling.
- Increased transient fission gas swelling.
- Microstructural changes in fuel clad material and in the liner (barrier) in the case of liner (barrier) *BWR* fuel.
- Development of a hydride rim at the clad outer surface (that may promote *PCMI* failures).
- Fuel design design changes resulting in up-rated duty on the clad.

Most sensitive component

Fuel cladding

Increase margin for *BWR*

- Ramp testing and hot cell *PIE* of high burnup fuel.
- Using 10x10 low *LHGR* fuel designs.
- Operating restrictions.
- Getting away from control cells and back to scatter loading.
- Using corrosion and hydride- resistant Zr alloy liners.
- Using pellets that are "soft" and with large grains.
- Control of pellet manufacturing parameters resulting in higher integrity pellets.

11 References

Adamson R. B., "*Effects of Neutron Irradiation on Microstructure and Properties of Zircaloy*", Zirconium in the Nuclear Industry; Twelfth International Symposium, ASTM STP 1354, ASTM, pp. 15-31, West Conshohocken, PA, 2000.

Adamson R. B. and Rudling P., "*Dimension Stability of Zirconium Alloys*", ZIRAT-7 Special Topical Report, 2002.

Adamson and Cox, "*Impact of Irradiation on Material Performance*", ZIRAT10 Special Topics Report, 2005.

Adamson R.B., Cox B., Garzarolli F., Riess R., Sabol G., Strasser A. and Rudling P., "*ZIRAT11 Annual report*", 2006.

Alam A. and Hellwig C., "*Stress Reorientation of Hydrides in Unirradiated Zircaloy-2 Specimens*", Conf. on Contribution of Materials Investigations to Improve the Safety and Performance of LWRs, Fontevraud, France, September, 2006.

Alam A. and Hellwig C., "*Cladding Tube Deformation Test for Stress Reorientation of Hydrides*", 15th Int. Symposium on Zirconium in the Nuclear Industry, ASTM, Sun River, OR, June, 2007.

Andersen J., Bolger F., Patterson C. and Robert C.,"*BWR LOCA Expected Impact of Proposed Requirements*", NRC-ACRS Meeting, Rockville, MD, January 19, 2007.

Andresen et al., Dissolved H2 Workshop, Tohoku University, July 2007.

Andersson T., Thorvaldson T., Wilson S. A. and Wardle A. M., "*Improvements in Water Reactor Fuel Technology and Utilization*", Proceedings of IAEA Symposium, Stockholm, Sweden, IAEA-SM-288/59, pp 435-449, 1987.

Anghel C., Hultquist G. Limbäck M and Szakalos P., "*Effects of Pt-coatings on Oxidation Resistance*", Paper presented at 15th Int. Symp. On Zr in the Nucl. Ind. , ASTM, Sun River, OR, 25-28th June, 2007.

Barberis P., Rebeyrolle V., Vermoyal J.J., Chabretou V. and Vassault, J.P., "*CASTA DIVTM: experiments and modeling of oxide induced deformation in nuclear components*", 15th ASTM International Symposium: Zirconium in the Nuclear Industry, Sun River, OR, June 2007.

Billone M., Yan Y. and Burtseva T., "*ANL Research Results Relevant to LOCA Embrittlement Criteria", Parts 1, 2 and 3*. ACRS Reactor Fuels Subcommittee Meeting, NRC, Rockville MD, January 19, 2007.

Blavius D., Mueuch E-J. and Garner N. L., "*Dimensional Behavior of Fuel Channels – Recent Experience and Consequences*", ANS/TOPFUEL, San Francisco, October, 2007.

Blat-Yrieix M., Ambard A., Foct F., Miguel A., Beguin S. and Cayet N., "*Toward a better understanding of dimensional changes in Zircaloy-4: What is the impact induced by hydrides and oxide layer?*", 15th Zirconium in the Nuclear Industry, ASTM, Sun River, OR, June 2007.

Bonacca M., *ACRS*, Letter to D. Klein, Chairman, USNRC, May 22, 2007.

Bossis P., Verhaeghe B., Doriot S., Gilbon D., Chabretou V., Dalmais A., Mardon J.P., Blat M. and Miquet A., "*In PWR Comprehensive Study of High Burn-up Corrosion and Growth Behaviorof M5 and Recrystallized Low-Tin Zircaloy-4*", 15th ASTM International Symposium: Zirconium in the Nuclear Industry – Sun River, OR, June 20, 2007.

Bouffioux P. and Rupa N., "*Impact of Hydrogen on Plasticity and Creep of Unirradiated Zry-4 Cladding Tubes*", Zirconium in the Nuclear Industry: Twelfth International Symposium, ASTM STP 1354, Sabol G. and Moan G., Eds., American Society for Testing and Materials, pp. 399-422, West Conshohocken, PA, 2000.

Bozzano P. B., Ipohorski M. and Versaci R. A., "*Pricipitate Evolution in Zry-4 Oxidation*", Paper presented at the IAEA/CNEA Technical Meeting on Behavior of High Corrosion Resistance Zr-Based Alloys, Buenos Aires, Argentina, October 24-27, 2005.

Brachet J.-C., Portier L., Forgeron T., Hivroz J., Hamon D., Guilbert T., Bredel T., Yvon P., Mardon J.-P. and Jacques P., "*Influence of Hydrogen Content on the α/β Phase Transformation Temperatures and on the Thermal-Mechanical Behavior of Zy-4, M4 (ZrSnFeV) and M5™ (ZrNbO) Alloys during the First Phase of LOCA Transient*", Zirconium in the Nuclear Industry: 13th Int'l Symposium, June 10-14, 2001, Annecy, France, ASTM STP 1423, Eds., American Society for Testing and Materials, West Conshohocken, PA, 2002.

Brachet J., Maillot V. Portier L., Gilbon D., Lesbros A., Waeckel N. and Mardon J-P., "Hydrogen Content, Pre-Oxidation and Cooling Scenario Influences on Post-Quench Mechanical Properties of Zy-4 and M5 Alloys in LOCA Conditions – Relationship with the Post-Quench Microstructure", 15th Int. Conf. on Zirconium in the Nuclear Industry, ASTM, Sun River, Oregon, June, 2007.

Buechel R. J., Moreno A. B., Young M. Y. and Mutyala M., "*Systematic Approach to PWR Fuel Performance Improvement*", Proceedings of the International Meeting on LWR Fuel Performance, Top_Fuel 2006, Salamanca Spain, European Nuclear Society, p. 143, 2006.

Cazalis B., Desquines C., Poussard C., Petit M., Monerie Y., Bernaudat C., Yvon P. and Averty X., "*The PROMETRA Program: Fuel Cladding Mechanical Behavior Under High Strain Rate*", Nuclear Technology, p. 215-229, vo. 157, March, 2007.

Choubey R., Aldridge S. A., Theaker J. R., Cann C. D. and Coleman C. E., "*Effects of Extrusion-Billet Preheating on the Microstructure and Properties of Zr2.5Nb Pressure Tube Materials*", Proc. 11th Int. Symp. on Zr in the Nucl. Ind., (E. R. Bradley and G. P. Sabol, Eds) ASTM-STP-1295, pp. 657-675., ASTM, 1996.

Clifford P., "*The US Nuclear Regulatory Commission's Strategy for Revising the RIA Acceptance Criteria*", Int. LWR Fuel Performance Meeting, San Francisco, California, September, 2007.

Coleman C. E. et al., "*Mechanical Properties of Zr-2.5 Nb Pressure Tubes Made From Electrolytic Powder*", Paper Presented at 15th Int. Symp. On Zr in the Nucl. Ind. Sun River, OR, 25-28th June, ASTM, 2007.

Cox B., "Hydrogen Absorption by Zircaloy-2 and Some Other Alloys During Corrosion in Steam", J. Electrochem. Soc., v. 109, pp 6-12, 1962.

Cox B., Chadd P. G. and Short J. F., "The Oxidation and Corrosion of Zirconium and its Alloys XV: Further Studies on Zirconium-Niobium Alloys", UKAEA Harwell, Report AERE-R4134, 1962.

Cox B. and Johnston T. J., "*The Oxidation and Corrosion of Niobium (Columbium)*", Trans.AIME, 227, pp. 36-42, 1963.

Cox B. and Read J. A., "*Oxidation of Zr-2.5 % Nb Alloy in Steam and Air*", UKAEA Harwell, Report AERE-R 4459, 1963.

Cox B., "A mechanism for the hydrogen uptake process in zirconium alloys", J. Nucl. Mater, Vol. 264, pp. 283-294, 1999.

Cox B. and Wong Y.M. "*A hydrogen uptake micro-mechanism for Zr alloys*", J. Nucl. Mat. Vol. 270, pp. 134-146, 1999.

Cui J., Shek G. K., Scarth D. A, Wang Z., "*Delayed Hydride Cracking Initiation at Simulated Debris Fretting Flaws in Zr-2.5 Nb Alloys*", Proc. ASME Pressure Vessels and Piping Division Conf., 23-27 July, Vancouver, BC Canada", 2006.

Delafosse J. and Poeydomange P., "*A Study of Zircaloy Type Alloys: Influence of Impuritieson Zircaloy-2 Water Corrosin and Mechanical Propterties*", Proc. 1st International Conference on Use of Zirconium Alloys in Nuclear Reactors, p. 121-134, Marianske Lazne, Skoda, Cz, 1968.

Delafoy C., Dewes P. and Miles T., "*AREVA NP Cr_2O_3-Doped Fuel Development for BWRs*", Int. LWR Fuel Performance Meeting, San Francisco, California, September, 2007.

del Barrio, M., Herranz, L., "FRAPTRAN Predictability of High Burnup Advanced Fuel Performance Analysis of the CABRI CIPO-1 and CIPO-2 Experiments", Int. LWR Fuel Performance Meeting, San Francisco, California, September, 2007.

Do T., Saidy M., and Hoocking W. H., "*Chemistry of water-side oxides on pressure tubes*", Presented at 15th Zirconium in the Nuclear Industry, ASTM, Sun River, OR, June 24-28, 2007, (to be published).

Domizzi G., Faba J., Garcia A., Goldbek V., Lanza H., Ruch M., Vizcaino P. and Belinco, C., "*Hydrogen Determination and Blister Detection in Zr-Alloys*", Paper presented at the IAEA/CNEA Technical Meeting on Behavior of High Corrosion Resistance Zr-Based Alloys, Buenos Aires, Argentina, October 24-27, 2005.

Donaldson A. T., "Growth in Zircaloy-4 fuel clad arising from oxidation at temperatures in the rage of 623 to 723 K", ASTM STP 1132, pp177-197, 1991.

Donavan K., INPO, Plenary Session Talk, Int. LWR Fuel Performance Meeting, San Francisco, California, September, 2007.

Doriot Sylvie, Gilbon Didier, Béchade Jean-Luc, Mathon Marie-Hélène, Legras Laurent and Mardon Jean-Paul, "*Microstructural Stability of M5TM Alloy Irradiated up to High Neutron Fluences*", (Proc: Proc: 14th Int. ASTM Symposium on Zr Alloys in Nuclear Industry, Stockholm, 2004.) Journal of ASTM International, 2005.

Dozaki et al., Dissolved H2 Workshop, Tohoku University, July 2007.

Dunn B., "*Comments on the Proposed Formulation of the Criteria and on Proceeding with the Rule Making Now*", NRC-ACRS Meeting, Rockville, MD, January 19, 2007.

Edsinger K., EPRI, Plenary Talk, Int. LWR Fuel Performance Meeting, San Francisco, California, September, 2007.

Eriksson J.H. and Hauffe K., "*The Influence on the Oxidation of Metals with Ionically Conducting Surface Layers of an Electrochemical Cell II Oxidation of Zirconium*", J. Phys. Chem. N.F., v 59, 332-340, 1968.

Forsberg S., Ahlberg E.L. and Limbäck M., "*Studies of Corrosion of Cladding Materials in Simulated BWR Environment Using Impendance Mesurements*", Paper presented at the 15th International Symposium on Zirconium in the Nuclear Industry, ASTM, Sun River, OR, June 28-25, 2007.

Fujii T., Teshima H., Kanasugi K., Kosaka Y. and Arakawa Y., "*Final Assessment of MOX Fuel Performance Experiment with Japanese PWR Specification Fuel in the HBWR*", Int. LWR Fuel Performance Meeting, San Francisco, California, September, 2007.

Fuketa T., Sugiyama T., Nagase F. and Suzuki M., "*JAEA Studies on High Burnup Fuel Behaviors During Reactivity-Initiated Accident and Loss-of-Coolant Accident*", Int. LWR Fuel Performance Meeting, San Francisco, California, October, 2007.

Garner G., Hilton B. and Mader E., "*Performance of Alloy M5 Cladding and Structure*", Int. LWR Fuel Performance Meetin, San Franciscom California, September, 2007.

Goll W., Hellwig Ch., Hoffmann P., Sauser W., Spino J. and Walker C., "*UO_2 Fuel Behavior at Rod Burnups to 105 MWd/kgHM*", Meeting on Status of LWR Fuel Development and Design Methods", FZ Rossendorf, Dresden, Germany, March, 2006.

Gregg R. and Worrall A., "*Effect of Highly Enriched/Highly Burnt UO_2 Fuels on Fuel Cycle Costs, Radiotoxicisity, and Nuclear Design Parameters*", Nuclear Technology, p. 126-132, Vol. 151, August, 2005.

Griffiths M., "*Microstructure Evolution in Zr-Alloys during Irradiation: Dose, Dose-rate and Impurity Dependence*", 15th ASTM International Symposium: Zirconium in the Nuclear Industry – Sun River, OR, June 20, 2007.

Foster J.P. and McGrath A.M., "*In-Reactor Creep Behavior of Zircaloy-2*", Proc: International LWR Fuel Performance Meeting, San Francisco, CA, September 30 to October 3, 2007.

Foster J., Yueh H. K. and Comstock, R.J., "*ZIRLO Cladding Improvement*", ASTM 15th International Symposium, Sun River, OR, June, 2007.

Garner G.L. et al., "*Performance of Alloy M5 cladding and structure*", Proc. 2007 Intern. LWR Fuel Performance Meeting, San Francisco, CA, 2007.

Garzarolli F., Steinberg E. and Weidinger H. G., "*Microstructure and Corrosion Studies for Optimized PWR and BWR Zircaloy Cladding*", Zirconium in the Nuclear Industry, 8th Int'l Symposium, ASTM STP 1023, Van Swam L. F. P. and Eucken C. M., Eds., ASTM, Philadelphia, 202-212, 1989.